

# **The fall and rise of V854 Centauri: long-term ultraviolet spectroscopy of a highly-active R Coronae Borealis star**

Warrick A. Lawson and Marco M. Maldoni

School of Physics, University College, Australian Defence Force Academy,  
Canberra ACT 2600, Australia;  
wal, mmmm@ph.adfa.edu.au

Geoffrey C. Clayton and Lynne Valencic

Department of Physics and Astronomy, Louisiana State University,  
Baton Rouge, LA 70803;  
gclayton, valencic@rouge.phys.lsu.edu

Albert F. Jones

Carter Observatory, P. O. Box 2903, Wellington, New Zealand;  
afjones@voyager.co.nz

and

David Kilkenny, Francois van Wyk, Greg Roberts and Fred Marang  
South African Astronomical Observatory, P. O. Box 9, Observatory 7935, South Africa;  
dmk, -, grr, -@sao.ac.za

Received \_\_\_\_\_; accepted \_\_\_\_\_

## ABSTRACT

We examine long-term low-dispersion *IUE* SWP and LWP spectroscopy of the R Coronae Borealis (RCB) star V854 Cen, obtained across the deep ( $\Delta V > 6$  magnitudes) 1991, 1992–1993 and 1994 declines. We also report the optical light curve for the star in the interval 1987–1998, including multi-color photometry obtained during 1989–1998. The light curve includes at least 8 major declines where the amplitude exceeds 5 magnitudes, many of which appear to be multiple decline events.

Analysis of the UV emission line spectra indicates most lines decay during the deep declines on characteristic timescales comparable to that reported for optical features. Fe, Mg and neutral C lines decay on timescales of typically 50–100 d. Other lines, notably ionized C lines, decay on longer timescales ( $> 200$  d) or appear to be unaffected by the declines. The general nature of the UV emission lines and other UV features during the declines is consistent with the E1/E2/BL line-region model developed from the behavior of optical spectral features during declines. However, the detailed line-behavior indicates large intrinsic variability between decline events inconsistent with the simple E1/E2/BL model. Limited temporal coverage prevents detailed examination of the geometry of the emission line region or the obscuring dust. We also report the first detection of the transition-region line C IV]  $\lambda 1550$  in the spectrum of an RCB star.

We fit the onset times of all declines from maximum light within the 1987–1998 interval, irrespective of decline amplitude, with a 43.23-d linear solution, thus improving the decline ephemeris of Lawson et al. (1992, MNRAS, 256, 347). The linear term is probably the pulsation period of V854 Cen, further supporting the suspected link between radial pulsations and mass loss in these types of stars.

*Subject headings:* stars: individual (V854 Cen) — stars: variables: other — stars: chemically peculiar — stars: coronae — ultraviolet emission

## 1. Introduction

The UV spectrum of an RCB star at maximum light closely resembles the UV spectra of late F-type supergiants. The most prominent features of the spectra are absorption lines of Mg II  $\lambda 2800$  and Fe II multiplets around 2400 and 2600 Å. The low resolution of most of the *International Ultraviolet Explorer (IUE)* spectra make line identifications difficult, particularly in the early-decline spectrum when many blended emission lines are present. Evans et al. (1985) attempted to identify the UV lines in an RY Sgr decline spectrum. Clayton et al. (1992a) identified many lines in the 1991 decline of V854 Cen. Holm et al. (1987) noted the similarity between the solar chromospheric spectrum and emission seen in the 1983 decline of R CrB. Table 3 of Clayton et al. (1992b) contains a line list prepared by comparing the decline emission spectra of RY Sgr, R CrB and V854 Cen.

Clayton et al. (1992b) summarized all previous spectroscopic work in the UV and visible on RCB stars, covering 10 declines of 3 RCB stars; R CrB, RY Sgr and V854 Cen. Most studies have involved observations of a small portion of a decline. In the visible spectral region, only the 1967 decline of RY Sgr (Alexander et al. 1972) and the 1988 decline of R CrB (Cottrell et al. 1990) had good coverage from early in the decline until the return to maximum light. Prior to the *IUE* observations reported in this paper, only the 1982–1983 and 1990–1991 declines of RY Sgr had reasonable coverage in the UV (Clayton et al. 1992b).

The general behavior of the emission spectrum in RCB declines is well known. As the photospheric light is extinguished by the forming dust cloud, a rich narrow-line emission spectrum appears. In the visible, this spectrum consists of many lines of neutral and singly ionized metals including Mg I, Si I, Ca I, Sc II, Ti II, V II, Cr II, Mn I, Fe I, Fe II, Sr II, Y II, La II, Ba II, and La II (Alexander et al. 1972; Payne-Gaposchkin 1963). Most of the lines in this spectrum, referred to as E1 (Alexander et al. 1972), are short-lived. Within a few days or weeks, most of these lines have faded and are replaced by a simpler broad-line ( $100\text{--}200 \text{ km s}^{-1}$ ) spectrum dominated by Ca II H and K, and Na I D. Some of the early-decline spectral lines remain strong for an extended period of time. These lines, also narrow and referred to as E2, are primarily multiplets of Sc II

and Ti II. In particular, the Sc II (7)  $\lambda 4246$  line remains strong. The E2 lines are primarily low excitation. There are many C I absorption lines which fill-in but never go into emission (Alexander et al. 1972). The Balmer lines, which are typically very weak due to the hydrogen deficiency in these stars, do not go into emission. The exception is in V854 Cen, which is much less hydrogen-deficient than the other RCB stars. V854 Cen shows strong Balmer line absorption at maximum light and emission in decline (Kilkenny & Marang 1989; Whitney et al. 1992). The late-decline spectrum is dominated by 5 strong broad-lines, Ca II H and K, the Na I D lines and a line at 3888 Å that may be He I. The broad-line (BL) emission spectrum remains visible until the star begins to return to maximum light and the photospheric continuum regains dominance.

The UV spectrum undergoes a very similar evolution to that in the optical (Clayton et al. 1992b). However, because all of the *IUE* observations during declines were made at low resolution, there is no information on the width of the emission lines. The UV spectral evolution is most clearly seen in the 1991 decline of V854 Cen (Clayton et al. 1992a) but can also be seen in the other UV declines. The very early-decline UV spectrum consists of blends of many emission lines, primarily multiplets of Fe II which make up a pseudo-continuum. The Mg II  $\lambda 2800$  doublet is present but not yet strong. The strong apparent absorption at 2650 Å is probably an absence of emission similar to that seen in the solar chromosphere (Holm et al. 1987). The actual photospheric continuum is the bottom of this apparent absorption feature. The V854 Cen spectrum is characterized by strong C II]  $\lambda 2325$  emission (Clayton et al. 1992a). With time, the early-decline spectrum begins to fade and be replaced by the late-decline spectrum. In the transition between these two spectral phases, there is still much blended emission but Mg II  $\lambda 2800$ , Mg I  $\lambda 2852$  and some of the Fe II lines have started to become relatively stronger. The late-decline spectrum is characterized by blended emission from multiplets of Fe II (2)  $\lambda 2400$ , Fe II (1)  $\lambda 2600$ , Fe II (62, 63)  $\lambda 2750$ , as well as from Mg II and Mg I. In addition, V854 Cen shows C I and C II] emission which is generally not seen in the other stars. Emission at C II  $\lambda 1335$  is visible at maximum light in R CrB and RY Sgr (Holm et al. 1987; Holm & Wu 1982). Rao, Nandy & Bappu (1981) report that emission is visible in Mg II in R CrB at maximum light.

The data presented here represent the most extensive coverage of an RCB star ever obtained in the UV during declines. 54 LWP low-resolution, 2 LWP high-resolution, and 13 SWP low-resolution spectra were obtained from the archive. Nearly half of these spectra were obtained when V854 Cen was 3 or more magnitudes below maximum light.

## 2. Observations and data reduction

SWP and LWP spectra of V854 Cen were obtained with the *IUE* satellite during 1991–1994. These are listed in Table 1, along with the FES and estimated visual magnitude of the star at the time of the *IUE* observation. Most of these data are large-aperture LWP and SWP low-resolution spectra. All these files have been reprocessed with NEWSIPS. Clayton et al. (1993) reported large-scale changes in UV line profiles in V854 Cen that appeared to be phased to the 43.2-d period of the star (Lawson et al. 1992). The NEWSIPS (and INES; Schartel & Skillen 1998) reduction of the *IUE* spectra shows no such effects. The line profile changes observed were likely an artifact of the previous reduction due to the low signal-to-noise, and nature (the spectra consist of weak emission lines with weak or absent stellar continuum) of these data.

The light curve of V854 Cen covering the interval 1987–1998, starting from near the discovery of the RCB-nature of the star (McNaught & Dawes 1986), is shown in Fig. 1. The star has been almost continuously monitored visually by one of us (AFJ) since discovery. Fig. 1 shows over 1600 visual estimates made with a 0.3-m telescope; the estimates obtained on average every 2.5 d. Sterken & Jones (1997) discuss the visual observing procedure. The uncertainty in the visual estimates is, at best, 0.1 mag, but can rise to 0.3–0.5 mag when the star is varying rapidly in brightness or color. Also, the visual estimates have an effective faint limit of  $V \approx 13.5$ .

Table 2 lists 323 sets of  $UBVR_cI_c$  photometry of V854 Cen obtained with the 0.5-m telescope at the South African Astronomical Observatory during 1989–1998. The measurements of V854 Cen were tied to observations of E-region photometric standards, and most of the  $V$  magnitudes and colors have  $1-\sigma$  uncertainties of  $< 0.01$  mag. Measurements of lower quality (normally when

the star is faint) are given to correspondingly lower precision in Table 2. The  $V$  light curve is shown in Fig. 1 and is discussed in Section 3.1; the color curves are shown in Fig. 2 and are discussed in Section 3.2.

Figs 1 and 2 also show decline onset-times used to improve the Lawson et al. (1992) decline ephemeris of V854 Cen, which we discuss in detail in Section 4. Fig. 3 shows the 1991–1994 photometry and visual estimates on an expanded scale. Note the generally good correspondence between the photoelectric and visual data, where these overlap. Times of the *IUE* LWP and SWP observations are indicated in both Figs 1 and 3.

### 3. Description of the observations

#### 3.1. Linking the light curve and the *IUE* spectra

The discovery decline (1987; commencing near JD6970; where Julian Dates are given as the difference JD–2440000) of V854 Centauri (then known as NSV 6708) was only observed visually. The 1988 decline (JD7400) was observed by Kilkenny & Marang (1989) and Lawson & Cottrell (1989), who obtained  $UBVRIJHKL$  photometry and visual spectroscopy. The 1989–1991 light curve has been discussed in detail by Lawson et al. (1992). The 1991 decline appeared to consist of three separate events (near JD8310, 8350 and 8395) with respective minima of  $V \approx 11, 14$  and 15. The first series of *IUE* spectra (1991; JD8335–8500) were acquired during the rise from the first fade, soon after the second minimum and throughout the deep third minimum. The final 1991 *IUE* spectra were made at  $V \approx 10.0$  as the star began to recover towards maximum light.

The star recovered to maximum light ( $V = 7.3$ ) only briefly near JD8610, before fading to  $V = 13.5$  by JD8750. Structure in the light curve is apparent during the initial decline (Fig. 3), with two partial recoveries near JD8700 and JD8730, then again at minimum near JD8810. The 1992 series of *IUE* spectra follow the decline from JD8650 ( $V = 7.7$ ) through JD8868 ( $V \approx 13$ ).

The star experienced a prolonged minimum until JD8980 (1993 January). There are no

photometric measurements from JD8850 until JD9030 by which time the star was  $V = 9.0$ . The few visual estimates made between JD8850–8980 indicate the star was highly-variable, and to have briefly reached  $V \approx 10$  near JD8960. There were no UV spectra during this period.

The star regained maximum light near JD9100. The rise to maximum, and the time at maximum light, was well-monitored in the UV; the 1993 series of *IUE* spectra consist of 27 observations made between JD9009–9217. High-resolution LWP spectra were obtained on JD9093 and JD9140 when V854 Cen was at, or near, maximum light (Lawson et al., in preparation). 1993 was the only year in the data set not characterised by the onset of a deep decline; however the star experienced a relatively long ( $\sim 200$  d) low-amplitude decline from JD9180–9350 that was unique in the 12-yr light curve.

The early-1994 light curve was characterised by the steepest decline in our data set. The  $V$  magnitude decreased from 7.5 (at JD9430) to 13 in  $\sim 20$  d. 11 *IUE* spectra were obtained during this time; from JD9427–9456. V854 Cen remained at minimum for  $\sim 30$  d before rising to  $V = 9$  near JD9530. The star subsequently faded again; slowly to  $V = 10$  near JD9600, then rapidly to  $V = 13.5$  near JD9620. The final 6 *IUE* spectra were obtained from JD9508–9539.

The remainder of the light curve was characterised by a major decline commencing in 1994 November (JD9860) with the star not fully-regaining maximum light until mid-1997 (near JD10600). Short-duration fades were seen near JD10345 and JD10775. The star entered a deep decline on JD10855 (1998 February).

### 3.2. The color curves

In Fig. 2 we present the color curves of V854 Cen from 1989–1998 (JD7500–11100). The colors during 1989–91 have been discussed by Lawson et al. (1992). The longer-term trends in the colors are similar to that already reported for this star and other RCB stars. For instance, in the 1990, 1991 and 1992 decline events, while the  $(U - B)$  decreased, the other colors reddened and varied in sympathy with the  $V$  curve (Figs 1 and 3). This effect is understood as the  $(U - B)$

index being ‘driven’ by the appearance of the emission line region which becomes prominent as the ejected dust cloud obscures the photosphere. Cottrell et al. (1990) observed that the  $(U - B)$  color turned blueward upon the appearance of the E1 emission spectrum during the 1988 decline of R CrB. Sometimes both the  $(U - B)$  and  $(B - V)$  colors decrease during the early stages of the decline before eventually reddening. Cottrell et al. (1990) termed these events ‘blue’ declines.

The 1994 and 1998 declines showed significant variations in the  $(U - B)$  color. The former decline is characterized by all the colors displaying blueward trends which correlate with the extreme nature of the event, i.e., a rapid decrease in visual light to  $V \sim 14$  in  $\sim 15$  d. Presumably the photosphere was obscured rapidly without significant obscuration of the emission line region. On JD9440, 10 d after the decline onset when the star was  $V = 13.4$ , the  $(U - B)$  color was 0.9 mag bluer (at  $-0.5$ ) than at maximum (0.4) and the  $(B - V)$  color was 0.5 mag bluer (0.0 *cf.* 0.5 at maximum). The next photometry was obtained at JD9485, by which time the star had recovered to  $V \approx 12$ .

The color behavior during the 1998 minimum differed in that the  $(U - B)$  and  $(B - V)$  colors become bluer during the decline minimum, at a time when the  $(V - R)$  and  $(V - I)$  colors were rapidly reddening. The  $(U - B)$  color peaked at  $-0.5$  on JD10947, when the star was  $V = 13.5$ ; 92 d after the decline onset at JD10855. Extreme color variations at minimum are probably due by the emergence of the optical BL spectrum (lines such as Ca H and K and Na D and broad continuum emission; see, e.g. Cottrell et al. 1990, figs. 2–4 and Clayton et al. 1993, fig. 2) as well as optical depth variations in the dust and coverage of the photosphere. However, the decline is not a ‘blue’ decline following the Cottrell et al. (1990) description.

Cottrell et al. (1990) also describe ‘red’ declines where both the photospheric and chromospheric fluxes are simultaneously reduced. This results in the color indices increasing, i.e. reddening. The 1992 decline appeared to show this trend. The initial behavior of the colors during the 1998 decline was also redward.

### 3.3. The UV spectrum evolution

A description of the UV spectrum of V854 Cen at maximum and minimum light was given by Clayton et al. (1992b). Lines of interest in the SWP and LWP spectra include C II  $\lambda$ 1335, C III]  $\lambda$ 1909 and C II]  $\lambda$ 2325, Fe II multiplets at  $\lambda$ 2400, 2600 and 2750, Mg II  $\lambda$ 2800, Mg I  $\lambda$ 2852 and C I  $\lambda$ 2965. Some of these are known to vary in strength as V854 Cen goes into a decline. Gross variations in the appearance of the SWP and LWP spectra are shown in Figs 4 and 5, where we show these spectral regions at maximum and minimum light. The NEWSIPS reduction has revealed the C IV]  $\lambda$ 1550 transition-region line for the first time in the spectrum of V854 Cen, and the only detection of this line in an RCB star. *IUE* spectra of RY Sgr and R CrB of similar signal-to-noise show no feature at this wavelength. Clayton et al. (1999) observed RY Sgr with STIS in the far-UV ( $\lambda\lambda$ 1140–1740 Å) and observed strong C II  $\lambda$ 1335 and Cl I  $\lambda$ 1351 emission, and possibly fluoresced CO emission pumped by C II  $\lambda$ 1335. There was no indication of C IV]  $\lambda$ 1550 in the STIS spectrum of RY Sgr.

The acquisition of UV data over an extended time span such as that covered by these observations may uncover long-term trends in the UV spectral evolution, particularly the quantitative changes in the strengths of the lines during declines. The long series of UV decline spectra of V854 Cen is unique for an RCB star, and is unlikely to be surpassed by current platforms such as *HST*.

Only a few measurements of ultraviolet emission-line strengths have been published. Herbig (1949) reported that the strength of the Ca II H and K lines of R CrB peaked as the star went into a decline and subsequently faded to one-fifth of their original strength. In contrast, the C II  $\lambda$ 1335 line in the same object was found to roughly remain constant during the 1983 decline at the same value measured at maximum light (Holm et al. 1987). Clayton et al. (1992b) provided further data concerning the strength of the Mg II emission line for the 1983 and 1988 decline of R CrB, the 1982 and 1990 decline of RY Sgr, and the early 1991 decline of V854 Cen. They found in R CrB that the line peak flux remained constant for 200 d into a decline, while in RY Sgr and V854 Cen the emission strength appeared to decrease after  $\sim$  100 d in a manner similar to that

observed by Herbig (1949) for the Ca II H and K lines in R CrB.

We have measured the peak line strengths in the *IUE* spectra of V854 Cen. Over the course of these observations (1991–1994) the C II  $\lambda 1335$ , C IV]  $\lambda 1550$ , C III]  $\lambda 1909$  and C II]  $\lambda 2325$  have average strengths of  $1 \times 10^{-14}$ ,  $7 \times 10^{-15}$ ,  $1 \times 10^{-14}$  and  $4 \times 10^{-14}$ , respectively, as seen at the *IUE* resolution (units are  $\text{erg s}^{-1} \text{cm}^{-2} \text{\AA}^{-1}$ ). The Fe II  $\lambda 2600$ , 2750 lines were at their maximum strengths during 1991 ( $8 \times 10^{-15}$  and  $5 \times 10^{-15}$ , respectively). Subsequently, throughout the data set, they were generally weaker than these values. The Mg I and Mg II lines, which were generally present during all minima, had respective maximum fluxes in 1991 of  $1.5 \times 10^{-14}$  and  $5 \times 10^{-15}$ . Finally, C I  $\lambda 2965$  had a similar maximum peak flux during 1991, 1992 and 1994 of  $4 \times 10^{-15}$ .

We have also measured the integrated flux (line intensities) of 9 key emission features in the SWP and LWP spectra except where the rising background continuum (at or near maximum light in the SWP spectra, and always present to some extent in the LWP spectra) made continuum-subtraction measurements unreliable. The line intensities of the C II  $\lambda 1335$ , C IV]  $\lambda 1550$  and C III]  $\lambda 1909$  lines (in the SWP spectra), and the C II]  $\lambda 2325$ , Fe II  $\lambda 2400$ , 2600, 2750, Mg II  $\lambda 2800$ , Mg I  $\lambda 2852$  and C I  $\lambda 2965$  lines (in the LWP spectra) are shown in Fig. 3 (units are  $\text{erg s}^{-1} \text{cm}^{-2}$ ). The uncertainty of a typical measurement is 10–20 percent; the uncertainty is contributed to by the choice of continuum placement and the quality of the flux calibration. Importantly, the trends seen in Fig. 3 agree with the visual assessment of the temporal evolution of the spectral features. Only large-aperture LWP spectra are measured because of the uncertain photometric corrections needed for the small-aperture observations. We have compared a number of SWP and LWP spectra extracted using both NEWSIPS and INES (Schartel & Skillen 1998) and find minimal differences in the appearance of the spectra and the emission line fluxes between the two reductions.

All the measured features are blends, and the intensities plotted in Fig. 3 represent the integrated flux of the blend, e.g. Fe II  $\lambda 2600$  consists of several weak Fe II lines with wavelengths ranging from 2586 to 2631 Å (see Fig. 5; some of these lines are resolved); Mg II  $\lambda 2800$  consists of a doublet at  $\lambda 2796$ , 2803. Wu et al. (1992; see table 1.1) identifies many of these blends. Clayton

(1992b; see table 3) list the presence of these lines across a number of declines for several RCB stars. There is no indication in the *IUE* spectra that the relative contribution of lines composing the blends changes as the blend intensity varies with time.

### 3.3.1. The 1991 decline

The 1991 decline (from JD8310) is characterised by 3 progressively deeper fades with the first *IUE* spectrum obtained near the first local minimum. All the LWP emission lines generally weakened during the interval JD8335–8500 (see Fig. 3). Line-intensity half-lives range from  $\sim 50$  d for Fe II  $\lambda 2750$ , Mg II  $\lambda 2800$  to  $\sim 200$  d for C II]  $\lambda 2325$  (see Fig. 6 and Table 3). Several features reached minimum strength at JD8436, in agreement with the time of the light curve minimum (Fig. 3). In particular, Fe II  $\lambda 2600$  increased in strength by a factor of  $\sim 4$  from the light of minimum light ( $V \approx 15$ ) as the star brightened to  $V = 10$ . Lines such as Fe II  $\lambda 2750$  continued to decay during this time. In contrast to general behavior of other LWP spectral lines, the Mg I  $\lambda 2852$  may have strengthened slightly as the star passed through the first 2 secondary minima and after the onset of the third minimum at JD8395. Thereafter, as the star faded to  $V = 15$ , the line intensity also rapidly decreased. In the 1991 SWP spectra, obtained after the decline minimum, all three key lines (C II  $\lambda 1335$ , C IV]  $\lambda 1550$  and C III]  $\lambda 1909$ ) appeared to remain constant.

### 3.3.2. The 1992–1993 decline

The 1992–1993 decline was the longest in our data set, lasting  $\sim 400$  d. Similar to many other declines of V854 Cen, this event shows multiple (in this case, 2) local minima between the onset of the decline from maximum light ( $V = 7.3$ ) at JD8610 and minimum ( $V \approx 14$ ) near JD8750. SWP and LWP spectra were obtained during the fade; other LWP spectra were obtained near minimum when the star brightened briefly to  $V = 12$  near JD8810. SWP and LWP spectra were obtained during the rise to maximum light during 1993, including 2 LWP high-resolution spectra.

The C II  $\lambda 1335$  line decayed by a factor of  $\sim 3$  during the fade. The behavior of the line is

unusual compared to the 1991 observations which showed the line to be bright (comparable to the intensity of the line at maximum light) even though the observations were made when the star was fainter than at any time during the 1992 decline. The next SWP observations were not made until JD9009, just prior to the star beginning to brighten towards maximum light; thus no SWP spectra were obtained across the 200 d minimum. During the rise, the C II  $\lambda$ 1335 line intensity was slightly ( $\sim$  50 percent) greater than when measured at the decline minimum. However, it remained a factor of  $\sim$  2 weaker than during 1991. C IV]  $\lambda$ 1550 may have been fainter during the decline minimum, based upon a single faint flux measurement at JD8787. C III]  $\lambda$ 1909 was insensitive to the decline and it remained at a level similar to that seen in 1991.

The LWP spectrum lines showed a variety of responses to the decline. C II]  $\lambda$ 2325 remained relatively constant and possibly stronger than in 1991. Fe and Mg lines were weak, but some brightened in sympathy with the 2 magnitude increase in visual flux near JD8820. (The actual rise in flux may have been somewhat greater than 2 magnitudes since the decline minimum was not well-observed photometrically and the visual estimates are unreliable below  $V \approx 13.5$ .) C I  $\lambda$ 2965 showed somewhat different behavior to that of the other lines. Measurements made during the final fade to minimum light in 1992 showed the line strength decreased from  $\sim 5 \times 10^{-14}$   $\text{erg s}^{-1}\text{cm}^{-2}$  to unmeasureably low ( $< 5 \times 10^{-15}$ ) between JD8720 and JD8724, and then regained its former strength by JD8792. At the time of the local maximum near JD8820, the line appeared to decrease in strength by 30–50 percent before recovering.

During the rise to maximum light during early-1993 (JD9000–) most LWP spectra are affected by the rising stellar continuum and the line strengths are unreliable or unmeasureable. However, on JD9009, most LWP lines had brightened above the average level measured near JD8800.

### 3.3.3. The 1994 decline

The 1994 decline was the most extreme of our data set, taking only  $\sim 16$  d for the star to fade from maximum light ( $V \approx 7.5$ ) at JD9430 to minimum ( $V \approx 13.50$ ) at JD9446. As in the previous

decline, the absence of photometric data through the decline minimum did not allow an accurate determination of the amplitude of the event. Visual estimates indicated the star remained at or below  $V = 13.5$  for  $\sim 30$  d. Subsequently, the star partly recovered (to  $V = 9$ , including a minor fade), which was then followed by another deep decline. Most of the LWP spectra acquired during 1994 were taken during the onset of the first decline with 3 LWP and 2 SWP spectra monitoring the recovery phase of the light curve. The SWP spectra showed that C IV]  $\lambda 1550$  and C III]  $\lambda 1909$  remained at a strength comparable to that during the 1991 and 1992–93 declines. However, the strength of C II  $\lambda 1335$  was similar to that during the 1992–93 decline. Presumably all the LWP line strengths decreased rapidly as the optical flux of V854 Cen faded towards minimum. This behavior was only observed in C II]  $\lambda 2325$ . Measurement of the line at JD9437 (7 d after the decline onset) gave an intensity of  $5 \times 10^{-13}$  erg s $^{-1}$  cm $^{-2}$ . By JD9449 (19 d after the decline onset) the line strength was comparable to the level recorded during the 1991 decline minimum ( $2.5 \times 10^{-13}$  erg s $^{-1}$  cm $^{-2}$ ). By JD9449, all other LWP spectral lines were weak. With the possible exception of Fe II  $\lambda 2600$ , all lines remained weak during the final series of *IUE* observations obtained as the star rose in brightness to  $V = 9$  by JD9540.

### 3.4. Summary of line behavior

Trends in the line strengths presented in Fig. 3 suggest that it may be possible to group some spectral lines according to their responses to a decline event. Clayton et al. (1992b) attempted to relate changes in the UV spectrum to those seen in the visible spectrum (Alexander et al. 1972, Cottrell et al. 1990). In their scheme, the ultraviolet E1, E2 and BL spectral features roughly correspond to their visible counterparts and were defined as:

E1 (fade in 10–30 d): Many blended lines of Fe II and other ionized metals, the apparent absorption feature at 2650 Å and weak Mg II  $\lambda 2800$ .

E2 (fade in 50–150 d): Most of the E1 lines have faded leaving Fe II multiplets at  $\lambda 2400$ , 2600 and 2750.

BL (fade but never disappear): Long-lasting lines of C II]  $\lambda$ 2325, Mg II  $\lambda$ 2800, Mg I  $\lambda$ 2852 and C I  $\lambda$ 2965.

In the 1991 decline, during the JD8300–8500 interval, C II  $\lambda$ 1335, C IV]  $\lambda$ 1550 and C III]  $\lambda$ 1909 are clearly BL as they show little change in strength during the decline minimum. C II]  $\lambda$ 2325 also probably originates in the BL emission region although it does weaken by  $\sim 50$  percent (Fig. 6).

The Fe II  $\lambda$ 2750, Mg II  $\lambda$ 2800, Mg I  $\lambda$ 2852 and C I  $\lambda$ 2965 lines all undergo significant decreases in intensity over the 170 day *IUE* coverage and thus are classified as E2 (Fig. 6). Mg I  $\lambda$ 2852 may be stronger near JD8400, in phase with the local maximum (Fig. 3). This may indicate that its region of origin is closer to the star than is the case for the other E2 lines. The behavior of Fe II  $\lambda$ 2600 is unusual as, unlike other E2 lines, it recovers strongly after only  $\sim 100$  d (Fig. 3). However, the decrease in intensity seen between JD8360–8466 is not rapid enough to classify the line as E1 and hence it is considered to be E2 (Table 3).

The only time an E1 LWP spectrum was obtained during 1991 was at JD8335. This spectrum looks similar to the early-decline spectra of RY Sgr and R CrB (Clayton et al. 1992a) as it showed a myriad of blended Fe II lines, apparent absorption at 2650 Å and Mg II  $\lambda$ 2800 substantially filled-in by emission. The first two E1 features were absent in the next LWP spectrum (JD8361) with Mg II  $\lambda$ 2800 being stronger (in emission) than at any other time in the data set. Clayton et al. (1992b) noted when there are several local minima, the E1 spectrum does not generally reappear, unless there is a long time between the local minima. During the 1991 decline, E1 features are only seen during the first local minimum. No *IUE* spectra were obtained between JD8500 (after the end of the 1991 minimum) and JD8650 (near the onset of the 1992–93 decline). During this time, the spectrum showed full recovery from one dominated by weak emission to one swamped by deep photospheric absorption. (Figs 4 and 5 show the gross changes in the SWP and LWP spectra from that at maximum light to the spectrum during the decline minimum.) Mg II  $\lambda$ 2800 best demonstrates the transition (Fig. 5). Visual inspection of the spectra (where line strengths could not be reliably measured) further supports the E2-type nature of this line.

The behavior of some of the lines during the 1992-93 decline shows the difficulty in trying to uniquely characterize their nature using emission-line decay times, e.g. the correlation between the light curve and the timescale for the decrease in C II  $\lambda$ 1335 is classic E2 (Table 3), unlike the BL appearance of this line in 1991. Inspection of Fig. 3 confirms the BL nature of C II]  $\lambda$ 2325 and C III]  $\lambda$ 1909; C IV]  $\lambda$ 1550 is probably BL. The timescales and appearance of the Mg lines suggest that these are E2 lines. Inspection of the LWP spectra shows that, during the multiple fade to minimum, Mg II  $\lambda$ 2800 emission progressively fills-in the deep Mg II  $\lambda$ 2800 absorption feature, but remains weak or absent and only becomes prominent during the decline minimum. During the rise to maximum light in 1993 it appeared as a weak emission feature on JD9009, whereas it was visible (in emission) at the bottom of a weak photospheric absorption at JD9045. Unlike the 1991 decline, the 2650 Å absorption feature was absent during this event.

The behavior of the Fe II  $\lambda$ 2600, 2750 and C I  $\lambda$ 2965 lines (Fig. 3) was more difficult to interpret. In particular, it was difficult to reconcile their changes in strength (and timescales) assuming the E1/E2/BL model. The rapid decay of C I  $\lambda$ 2965 at JD8720 is compatible with E1-type behavior. No other LWP lines showed this rapid response to the decline minimum. These lines show rapid and discordant behavior during the local maximum near JD8820. Fe II  $\lambda$ 2720 appeared to peak at JD8829; whereas C I  $\lambda$ 2965 decreased in strength by a factor of  $\sim 2$  near JD8829/8835. Both lines recover their pre-JD8829 fluxes by JD8868. The timescales of both lines are more suggestive of E1 than E2. Fe II  $\lambda$ 2600 showed little or no reaction to the local minimum.

Finally, measurements made during the 1994 decline presented a similar classification dilemma to that discussed above. In this event, all SWP lines remained at strengths similar to that observed during previous declines, and thus are BL, but all LWP lines faded rapidly and apparently in phase with the light curve. The decrease in the line intensity was only measured in CII]  $\lambda$ 2325 (Fig. 3 and Section 3.3.3) on timescales (the line faded by a factor of 2 in 20 d) consistent with E1 behavior, when the line either showed long-E2 or BL behavior during 1991-93. By JD9449, 19 d after the decline onset, all LWP lines were faint at levels similar to that observed during the 1991 and 1992-93 decline minima (Fig. 3). Thus we would conclude from the apparent timescales for

the fading of these lines that all these features are E1, if it were not for the combined photometric and spectroscopic evidence that the 1994 decline was particularly rapid compared to the other declines. The color curves (Fig. 2) indicate that the  $(U - B)$  color was 0.9 mag bluer than at maximum at JD9440, only 10 d after the decline onset – evidence that the photosphere was rapidly obscured, exposing the emission line region. The LWP spectrum obtained on JD9449 indicated that the emission line region was then obscured on a timescale of  $< 9$  d. From inspection of the LWP spectra, we can also estimate that it took  $< 19$  d after the decline onset for the 2650 Å feature to disappear and for the Mg II  $\lambda 2800$  absorption line to weaken and fill-in, and then go into emission.

In summary – while the emission line behavior across several declines of V854 Cen was generally in agreement with the E1/E2/BL model, the behavior is more complex than the simple model predicts. Temporal coverage of the declines is insufficient to discern the geometry of the emission line regions and that of the eclipsing dust, e.g. UV Mg lines were expected to behave like optical BL lines (such as Ca II H and K, and Na I D) but instead showed more-rapid activity commensurate with E1 and E2 lines. As more data is obtained of these types of events, we expect these stars and their individual declines will probably show large intrinsic variation in the nature of the emitting region and the eclipsing dust cloud.

#### 4. A revised pulsation-decline ephemeris for V854 Cen

Lawson et al. (1992) discovered a link between decline onset times and the probable pulsation period of the star, with 8 decline onset times between JD6970 (1987) and JD8395 (1991) being fitted by the linear solution:

$$JD_n = 2447400.6 (\pm 1.1) + 43.2 (\pm 0.1) n \text{ d},$$

between cycle numbers  $n = -10$  and 23.

The ephemeris fitted the onset times of the 1987 (JD6970,  $n = -10$ ) and 1988 (JD7400,  $n = 0$ ) declines, two low-amplitude fades and one large-amplitude decline in 1989 (JD7705, 7785

and 7875;  $n = 7, 9$  and  $11$ , respectively), and the triple 1991 decline (JD8310, 8350 and 8395;  $n = 21, 22$  and  $23$ , respectively). The ephemeris also appeared to satisfy times of maxima on the light curve during 1989 that may be due to low-amplitude pulsations of the star. If this is the case, V854 Cen is similar to the RCB star RY Sgr, which has pulsation maxima and decline onset times tied to a 37.8-d period (Pugach 1977). A 43-day pulsation period for V854 Cen would be entirely consistent with the pulsation period of other RCB stars of similar  $T_{\text{eff}}$  most of which have pulsation periods of  $\sim 40$  d (Lawson et al. 1990, Lawson & Cottrell 1997).

With the light curve from 1987–1998 available to us (Fig. 1), we have extended the Lawson et al. decline ephemeris across the entire data set. We fit the onset times (15 epochs) of *all* declines from maximum light ( $V \approx 7.5$ ; 13 epochs) within the 1987–1998 interval, irrespective of decline amplitude, and the last 2 fades of the triple 1991 decline (the first fade occurred from maximum light and is included in the 13 epochs above; the other two fades occurred from  $V \approx 10$ ), with the linear solution:

$$\text{JD}_n = 2447400.43 (\pm 1.33) + 43.23 (\pm 0.03) n \text{ d},$$

between cycle numbers  $n = -10$  and  $80$ .

The 15 epochs are indicated in Fig. 1, and some are shown in Figs 2 and 3 where the epochs extend across the interval observed photometrically. The revised solution is in agreement with the Lawson et al. (1992) ephemeris to within the respective uncertainties of the two solutions. Table 4 lists the observed epochs, calculated epochs from the ephemeris, and the observed–calculated (O–C) residuals. Figure 7 plots the O–C residuals as a function of period number, and binned as a histogram. The  $1-\sigma$  scatter of all 15 residuals is 3.3 d. The earlier ( $n = -10$  to 28) residuals determined mainly from photoelectric measurements have lower scatter ( $1-\sigma = 2.1$  d) than the later residuals ( $n = 41$  to 80,  $1-\sigma = 4.9$  d) which are determined mainly from the visual estimates. However, all of these  $1-\sigma$  values are similar to the typical uncertainty in the observed decline onset time of  $\pm 5$  d. There is currently no evidence for higher-order, e.g. quadratic, terms in the ephemeris, as has been claimed for RY Sgr (Kilkenny 1982, Marraco & Milesi 1982).

Most of the declines showed complex structure in the light curve as the star faded from maximum light, with several local maxima giving the appearance of multiple decline events. Only in the 1991 decline (commencing JD8310) did the times of the local maxima seen during the fade (JD8350, 8395) support both the Lawson et al. (1992) and revised ephemerides. Some of the structure seen during declines was approximately fitted by the revised ephemeris. In a number of declines, local maxima seen during the initial fade, and during the decline minima, gave an O–C residual of  $-10$  to  $-15$  d, i.e. the features had ‘maxima’ that occurred 10–15 d before the ephemeris prediction. Such features occurred during the 1992 (near JD8690, 8725, 8815), 1994 (JD9540, 9590) and 1998 (JD10885, 10930) declines. The apparent connection between these times and the ephemeris, only offset by 10–15 d, suggests they are also linked in some way to the 43.23 d periodicity.

## 5. Discussion

### 5.1. Dust formation in RCB stars

The traditional model for the declines in RCB stars considers the homogenous nucleation of carbon particles in thermodynamic equilibrium at temperatures of  $\sim 1500$  K and at a distance of  $\sim 20R_*$  (see, e.g. Feast 1986). Radiation pressure slowly dissipates the dust cloud.

Over the past 10 years, a wealth of observational and theoretical evidence has pointed increasingly towards dust formation in the near-star field, at distances of  $\sim 2R_*$ . For example, (i) simultaneous optical photometry and spectroscopy indicates the dust cloud can initially obscure only part of the photosphere. The cloud can then be rapidly accelerated away from the star by radiation pressure. The photosphere is obscured on timescales of typically 10–20 d, revealing a rich emission line region of which the inner regions (the E1 spectral region) are obscured in a further 10–20 d (Cottrell et al. 1990, Lawson 1992). The timescale of the fade to minimum light of 30–50 d, followed by recovery on timescales of hundreds of days, can be modelled by radial expansion at  $100\text{--}200\text{ km s}^{-1}$  of an obscuring cloud from a point of close proximity to

the star. The expansion velocity is consistent with that of blue-shifted absorption features seen during declines (Alexander et al. 1972, Cottrell et al. 1990, Clayton et al. 1993). (ii) The decay timescales for lines formed in the emission region suggests the E1 region has an extent of 1.5–2  $R_\star$ , the E2 region is  $\sim 5$  times larger, and the BL region is larger still. The available evidence suggests at least 2 temperature regimes in the emission line region; a cool ( $\sim 5000$  K; Clayton et al. 1992a) inner region likely to be the site of neutral and singly-ionized species composing the E1 and E2 spectrum, and a much hotter outer region indicated by the presence of BL lines such as C III]  $\lambda 1909$ , C IV]  $\lambda 1550$  and He I  $\lambda 10830$ . The presence of C IV]  $\lambda 1550$  implies the presence of a transition region with an electron temperature  $T_e \sim 10^5$  K (Jordan & Linsky 1987). (iii) The linking of decline onset times and pulsation periods in RY Sgr (Pugach 1977) and V854 Cen (Section 4) is only possible if dust formation is intimately associated with the pulsations of the star, with little phase delay between the time of maximum light on the pulsation cycle and the onset of the decline. Clayton et al. (1992b) reviewed empirical evidence for dust formation near the stellar surface.

More recently, (iv) Woitke, Goeres & Sedlmayr (1996) produced models that suggested the presence of (pulsation-induced) shocks in the outer atmosphere of a hydrogen-deficient star might result in conditions far-removed from thermodynamic equilibrium, encouraging particle nucleation. Such photospheric shocks are observed in the RCB star RY Sgr (Lawson, Cottrell & Clark 1991, Clayton et al. 1994) and may be present in other RCB stars. (v) Lawson & Cottrell (1997) showed all well-observed RCB stars were pulsating stars, and (vi) Clayton et al. (1999) reported the probable discovery in RY Sgr of CO, critical to the Woitke et al. (1996) model. Polar molecules such as CO play a major role in gas radiative heating and cooling. In hydrogen-deficient atmospheres, CO is expected to be the most abundant polar molecule by two orders of magnitude.

To this evidence, measurement of UV emission lines in V854 Cen shows some consistency with the E1/E2/BL model developed from the behavior of the optical spectrum during declines. Although we have poor sampling near the times of decline onset, the few E1 spectra obtained suggest characteristic E1 lines decay on timescales of several tens of days (see Section 3.4).

E2-region lines in 1991 decay on timescales of 50–120 d (see Section 3.3.1). BL-region lines throughout the data set generally decay on timescales of hundreds of days (e.g. C II  $\lambda$ 1335). Some lines may be ‘super-BL’ (coronal and transition-region lines such as C III]  $\lambda$ 1909 and C IV]  $\lambda$ 1550) and remain essentially constant despite the high-degree of activity seen in the V854 Cen light curve.

Uniquely for an RCB star, we have analysed spectroscopy across several consecutive major declines of V854 Cen. Emission line decay timescales clearly differ between declines. This can be related to probable free parameters such as the initial size and extent of the obscuring cloud, ejection velocity and future evolution of the cloud, and axis of the cloud motion with respect to the line-of-sight (e.g. Pugach 1990). Hardly surprising, the E1/E2/BL scheme needs to be interpreted as a simple classification scheme for characterising the evolution of the post-decline spectrum, where decay timescales and the behavior of individual lines should be seen only as indicative.

## 5.2. Dust formation in other types of cool hydrogen-deficient carbon stars

Recent analysis of *IUE* spectra of other hydrogen-deficient carbon stars has revealed possible differences between the RCB stars and the (optically) spectroscopically-similar HdC stars (Lambert 1986). Brunner, Clayton & Ayres (1998) found no evidence of C II  $\lambda$ 1335 in the HdC star HD 182040, whereas the line is present at all times in the UV spectrum of V854 Cen (Fig. 4), R CrB (Holm et al. 1987) and RY Sgr (Clayton et al. 1999). The line may also be absent in XX Cam (Brunner et al. 1998), which has been classified as both RCB and HdC star, but has no bright-IR excess like HD 182040. Absent or weak C II  $\lambda$ 1335 may be an important discriminator between RCB and HdC stars. Lawson & Cottrell (1997) found that the HdC stars are either low-amplitude pulsators, or that they are not pulsating above a 1- $\sigma$  radial velocity limit of  $\sim 1.5 \text{ km s}^{-1}$ . Only 1 of 5 HdC stars measured by Lawson & Cottrell, HD 175883, was found to have a photometric and radial velocity amplitude comparable to the RCB stars. HD 175893, along with HD 173409, was suspected of having a weak (compared to RCB stars) infrared excess in *IRAS* 12- $\mu\text{m}$  photometry (Walker 1986). *ISO* 12- and 25- $\mu\text{m}$  photometry confirms that only the excess in HD 175893 is real

(Lawson et al., in preparation). Pulsations in these types of stars seem responsible for encouraging mass-loss in the form of high-velocity outflows and dust, but only if the radial velocity amplitude exceeds  $10\text{--}15 \text{ km s}^{-1}$  peak-to-peak. The dust and gas may be linked by the presence of  $200\text{--}400 \text{ km s}^{-1}$  blue-shifted absorption seen during the declines (Alexander et al. 1972, Cottrell et al. 1990, Clayton et al. 1993). This may be gas being dragged away from the star by the ejected dust cloud. Gas density enhancement in the BL region due to enhanced mass-loss in RCB stars, compared to HdC stars, may be responsible for the strong C II  $\lambda 1335$  emission.

### 5.3. V854 Cen as a pulsating star?

All well-observed RCB stars are pulsating stars. Most RCB stars with  $T_{\text{eff}}$  similar to V854 Cen (such as RY Sgr and R CrB;  $T_{\text{eff}} \approx 7000 \text{ K}$ ), have a radial velocity-to-light (RV/V) amplitude ratio of  $\approx 50 \text{ km s}^{-1} \text{ mag}^{-1}$ , similar to radially-pulsating Cepheids (Lawson & Cottrell 1997). Typical amplitudes (peak-to-peak) are  $10\text{--}15 \text{ km s}^{-1}$  in radial velocity and  $0.2\text{--}0.3$  in  $V$ , although RY Sgr is more active ( $30\text{--}40 \text{ km s}^{-1}$  and  $0.5\text{--}0.7$  mag, respectively).

So far, it has not been possible to reliably measure pulsation amplitudes for V854 Cen, due to the extreme nature of the light curve of the star, and the likely low-amplitude of the pulsations. Some observations at maximum in the 1989–1991 light curve (Lawson et al. 1992) showed semi-regular variations on timescales of  $\sim 40\text{-d}$  and with amplitudes of  $0.1\text{--}0.2$  mag that are probably due to radial pulsations. Lawson & Cottrell (1989) did not detect radial velocity variations in a short series of measurements made in 1988, but the individual measurements had  $1\text{-}\sigma$  uncertainties of  $3\text{--}5 \text{ km s}^{-1}$ . If  $\text{RV}/V \approx 50$  for V854 Cen, like other RCB stars, then the radial velocity amplitude is expected to be only  $\sim 10 \text{ km s}^{-1}$ .

The onset times of declines in V854 Cen are satisfied by a  $42.23 \text{ d}$  period, which is probably the pulsation period of the star. Other RCB stars of similar  $T_{\text{eff}}$  have similar periods (Lawson et al. 1990, Lawson & Cottrell 1997). It remains unresolved why V854 Cen is currently more active than other RCB stars. The greater hydrogen abundance in V854 Cen, compared to any other

known RCB star, may encourage dust production. However, other RCB stars are known to have experienced prolonged intervals of dust production in the past.

WAL thanks the University College ADFA Special Research Grant Scheme, and Department of Physics and Astronomy at LSU for financial support. WAL and MMM thank the Australian Research Council Small Grant Scheme FY97 for supporting this research. GCC was supported by NASA grant JPL 961526.

## REFERENCES

Alexander, J. B., Andrews, P. J., Catchpole, R. M., Feast, M. W., Lloyd Evans, T., Menzies, J. W., Wisse, P. N. J., & Wisse, M. 1972, MNRAS, 158, 305

Brunner, A. R., Clayton, G. C., & Ayres, T. R. 1998, PASP, 110, 1412

Clayton, G. C., Whitney, B. A., Stanford, S. A., Drilling, J. S., & Judge, P. G. 1992a, ApJ, 384, L19

Clayton, G. C., Whitney, B. A., Stanford, S. A., & Drilling, J. S. 1992b, AJ, 397, 652

Clayton, G. C., Lawson, W. A., Whitney, B. A., & Pollacco, D. L. 1993, MNRAS, 264, L13

Clayton, G. C., Lawson, W. A., Cottrell, P. L., Whitney, B. A., Stanford, S. A., & de Ruyter, F. 1994, ApJ, 432, 785

Clayton, G. C., Ayres, T. R., Lawson, W. A., Drilling, J. S., Woitke, P., Asplund, M. 1999, ApJ, in press

Cottrell, P. L., Lawson, W. A., & Buchhorn, M. 1990, MNRAS, 244, 149

Evans, A., Whittet, D. C. B., Davies, J. K., Kilkenny, D. , & Bode M. F. 1985, MNRAS, 217, 767

Feast, M. W. 1986, Hydrogen Deficient Stars and Related Objects, K. Hunger, Dordrecht: Reidel, 151

Herbig, G. H. 1949, ApJ, 110, 143

Holm, A. V., Hecht, J., Wu, C. -C., & Donn, B. 1987, PASP, 99, 497

Holm, A. V., & Wu, C. -C. 1982, Advances in Ultraviolet Astronomy: Four Years of *IUE* Research, Y. Kondo, J. Mead and R. C. Chapman, Washington, DC: NASA, 429

Jordan, C., & Linsky, J. L. 1987, Exploring the Universe with the *IUE* satellite, Y. Kondo, Dordrecht: Kluwer, 259

Kilkenny, D. 1982, MNRAS, 200, 1019

Kilkenny, D., & Marang, F. 1989, MNRAS, 238, 1P

Lambert, D. L. 1986, Hydrogen Deficient Stars and Related Objects, K. Hunger, Dordrecht: Reidel, 127

Lawson, W. A. 1992, MNRAS, 258, 1P

Lawson, W. A., & Cottrell, P. L. 1989, MNRAS, 240, 689

Lawson, W. A., & Cottrell, P. L. 1997, MNRAS, 285, 266

Lawson, W. A., Cottrell, P. L., Gilmore, A. C., & Kilmartin, P.M. 1990, MNRAS, 247, 91

Lawson, W. A., Cottrell, P. L., & Clark, M. 1991, MNRAS, 251, 687

Lawson, W. A., Cottrell, P. L., Gilmore, A. C., & Kilmartin, P.M. 1992, MNRAS, 256, 339

Marraco, H. G., & Milesi, G. E. 1982, AJ, 87, 1775

McNaught, R., & Dawes, G. 1986, IAU Circ. 4233

Payne-Gaposchkin, C. 1963, ApJ, 138, 320

Pugach, A. F. 1977, Info. Bull. var. Stars, No. 1277

Pugach, A. F. 1990, AZh, 67, 1280

Rao, N. K., Nandy, K., & Bappu, M. K. V. 1981, MNRAS, 195, 71P

Schartel, N., & Skillen, I. 1998, UV Astrophysics, Beyond the IUE Final Archive, W. Wamsteller and R. Gonzalez Riestra, ESTEC: Noordwijk, 735

Sterken, C., & Jones, A. F. 1997, J. Astron. Data, 3, 4

Walker, H. J. 1986, Hydrogen Deficient Stars and Related Objects, K. Hunger, Dordrecht: Reidel,

Whitney, B. A., Clayton, G. C., Schulte-Ladbeck, R. E. , & Meade, M. R. 1992, AJ, 103, 1652

Woitke, P., Goeres, A., & Sedlmayr, E. 1996, A&A, 313, 217

Wu, C. -C., Reichert, G. A., Ake, T. B., Boggess, A., Holm, A. V., Imhoff, C. L., Kondo, Y., Mead, J. M. , & Shore, S. N. 1982, International Ultraviolet Explorer (*IUE*) Ultraviolet Spectral Atlas of Selected Astronomical Objects, Washington, DC: NASA, 4

Fig. 1.— Visual and photoelectric  $V$  light curve for V854 Cen from 1987–1998. Times of the *IUE* SWP and LWP spectra are indicated. Also shown are calculated decline onset times from the pulsation-decline ephemeris derived in Section 4.

Fig. 2.— Color curves for V854 Cen from 1989–1998, including decline onset times over this interval.

Fig. 3.— The 1991–1994 light curve for V854 Cen on an expanded scale, with times of the *IUE* SWP and LWP spectra indicated (top panel), and integrated line fluxes (line intensities) for key emission features in the SWP and LWP spectra (lower panels). Line intensity units are  $\text{erg s}^{-1} \text{cm}^{-2}$ . Some measurements could not be made due to the intrusion of bright stellar continuum (usually when the star was at or near maximum light). The vertical bar in the lower-right corner of the panel for each emission line indicates a nominal uncertainty of  $\pm 20$  percent in the line intensities, based upon the average flux for each line (see Section 3.3 for further discussion of the uncertainties).

Fig. 4.— (upper) Sample SWP spectra of V854 Cen obtained at maximum and minimum light. (lower) Average of SWP spectra of V854 Cen obtained at minimum, constructed by co-adding the 5 long-exposure ( $> 12$  ks) spectra obtained during declines that are without significant photospheric absorption longward of 1500 Å, weighted by exposure time. Key emission features are labelled.

Fig. 5.— Sample LWP spectra of V854 Cen obtained at maximum (upper) and minimum light (lower, where the re-scaled bright spectrum is also shown for comparison). Key absorption and emission features are labelled.

Fig. 6.— Decay of the LWP emission lines during the 1991 decline. The lines are exponential fits to the emission line intensities. Decay time-scales (half-lives) for the emission lines range from 50–200 d (see Section 3.3.1 and Table 3). A nominal uncertainty of  $\pm 20$  percent in the average line intensity of the LWP lines is indicated in the upper panel.

Fig. 7.— (upper) Observed–Calculated (O–C) residuals versus cycle number for the pulsation-decline ephemeris for V854 Cen. (lower) O–C residuals plotted as a histogram.

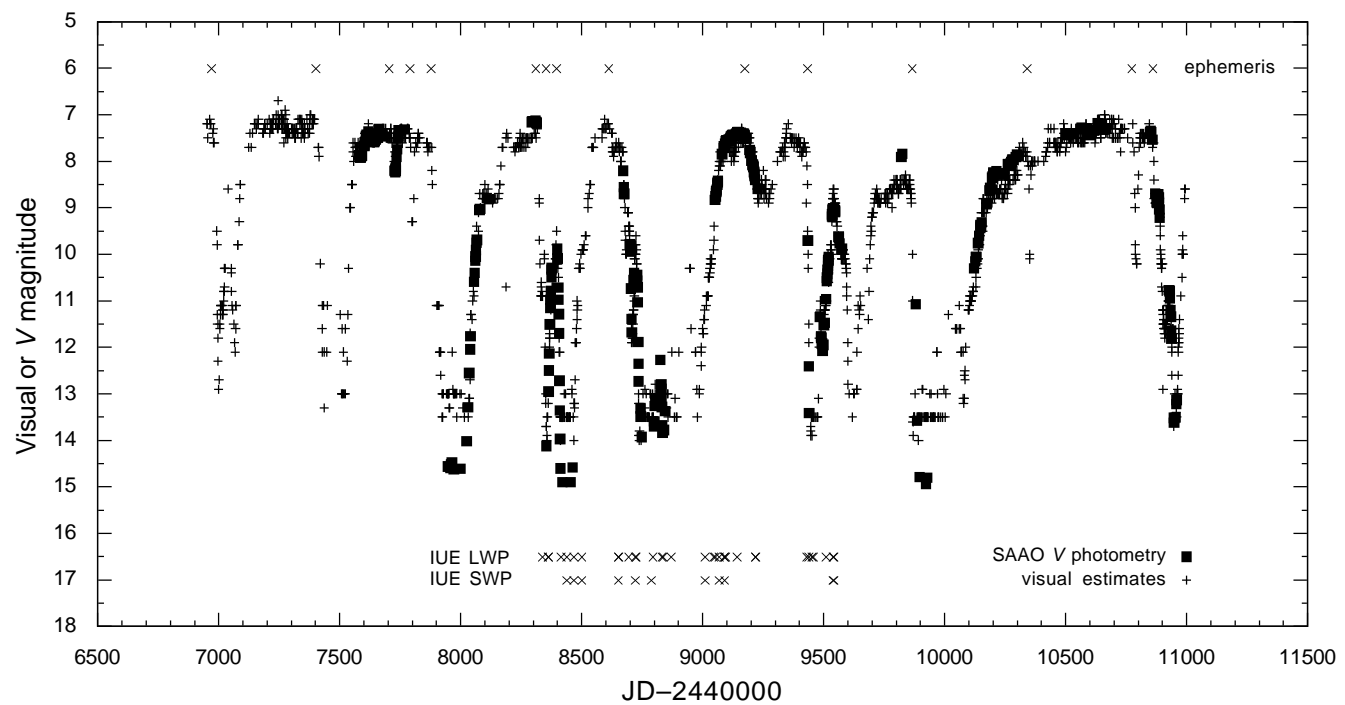


TABLE 1. IUE spectra of V854 Centauri.

| JD-2440000 | Date     | $V_{\text{FES}}$ | $V_{\text{AFJ}}$ | Image No. | Exp. (s) | Notes             |
|------------|----------|------------------|------------------|-----------|----------|-------------------|
| 8335.437   | 19/03/91 | 10.396           | 10.8             | LWP 19951 | 9899     |                   |
| 8335.571   | 20/03/91 | 10.418           | 10.8             | LWP 19951 | 3900     | small aperture    |
| 8360.916   | 14/04/91 |                  | 12.9             | LWP 20141 | 24600    |                   |
| 8361.906   | 15/04/91 | 13.349           | 12.9             | LWP 20150 | 12600    |                   |
| 8412.788   | 05/06/91 |                  | 13.5             | LWP 20527 | 21600    |                   |
| 8436.758   | 29/06/91 |                  | 13.5             | SWP 41954 | 14400    |                   |
| 8436.932   | 29/06/91 |                  | 13.5             | LWP 20710 | 9000     |                   |
| 8466.019   | 28/07/91 | 12.996           | 13.2             | LWP 20899 | 3600     |                   |
| 8466.090   | 28/07/91 |                  | 13.2             | SWP 42136 | 3900     |                   |
| 8466.139   | 28/07/91 | 12.866           | 13.2             | LWP 20900 | 12600    |                   |
| 8499.909   | 31/08/91 | 9.992            | 10.0             | LWP 21126 | 10800    |                   |
| 8500.057   | 31/08/91 | 9.993            | 10.0             | SWP 42366 | 12300    |                   |
| 8650.351   | 28/01/92 | 8.269            | 7.7              | LWP 22293 | 12600    |                   |
| 8650.398   | 28/01/92 | 8.307            | 7.7              | SWP 43888 | 6600     |                   |
| 8651.429   | 29/01/92 | 8.201            | 7.7              | LWP 22301 | 3780     |                   |
| 8692.976   | 11/03/92 | 9.266            | 9.2              | LWP 22570 | 5399     |                   |
| 8720.060   | 07/04/92 | 10.027           | 10.1             | LWP 22761 | 4800     |                   |
| 8720.119   | 07/04/92 | 10.023           | 10.1             | SWP 44351 | 7200     |                   |
| 8724.068   | 11/04/92 | 9.948            | 9.8              | LWP 22788 | 10799    |                   |
| 8786.751   | 13/06/92 |                  | 13.3             | SWP 44920 | 24300    |                   |
| 8792.771   | 19/06/92 |                  | 13.2             | LWP 23324 | 22800    |                   |
| 8829.574   | 26/07/92 | 11.139           | 13.1             | LWP 23584 | 25200    |                   |
| 8835.588   | 01/08/92 |                  | 13.1             | LWP 23610 | 5100     |                   |
| 8835.780   | 01/08/92 |                  | 13.1             | LWP 23611 | 19200    |                   |
| 8868.484   | 02/09/92 |                  |                  | LWP 23833 | 25800    |                   |
| 9009.367   | 21/01/93 |                  | 11.2             | LWP 24767 | 9300     | *                 |
| 9009.479   | 21/01/93 |                  | 11.2             | SWP 46793 | 9300     |                   |
| 9045.083   | 26/02/93 | 8.218            | 9.6              | LWP 25011 | 5400     | *                 |
| 9045.186   | 26/02/93 | 8.311            | 9.6              | LWP 25012 | 7200     | *                 |
| 9045.186   | 26/02/93 | 8.311            | 9.6              | LWP 25012 | 7200     | small aperture, * |
| 9045.296   | 26/02/93 | 8.427            | 9.6              | LWP 25013 | 6300     | *                 |
| 9051.004   | 04/03/93 | 8.140            | 8.8              | LWP 25057 | 3600     | *                 |
| 9051.072   | 04/03/93 | 8.137            | 8.8              | LWP 25058 | 8100     | *                 |
| 9051.234   | 04/03/93 | 8.118            | 8.8              | LWP 25059 | 8400     | *                 |
| 9067.325   | 20/03/93 | 8.171            | 8.2              | LWP 25159 | 3600     | *                 |
| 9067.370   | 20/03/93 | 8.225            | 8.2              | SWP 47326 | 3600     |                   |
| 9067.415   | 20/03/93 | 8.249            | 8.2              | LWP 25160 | 1800     | *                 |
| 9067.439   | 20/03/93 | 8.228            | 8.2              | SWP 47327 | 11400    |                   |
| 9067.574   | 21/03/93 | 8.227            | 8.2              | LWP 25161 | 3600     | *                 |
| 9088.923   | 11/04/93 | 7.635            | 7.7              | LWP 25319 | 7200     | *                 |
| 9089.013   | 11/04/93 | 8.228            | 7.7              | SWP 47461 | 10800    |                   |
| 9089.144   | 11/04/93 |                  | 7.7              | LWP 25320 | 900      | *                 |
| 9089.163   | 11/04/93 |                  | 7.7              | SWP 47462 | 3600     |                   |
| 9093.920   | 16/04/93 |                  | 7.7              | LWP 25355 | 24600    | high dispersion   |
| 9140.735   | 02/06/93 | 7.399            | 7.6              | LWP 25658 | 25800    | high dispersion   |
| 9215.586   | 16/08/93 | 7.574            | 8.4              | LWP 26157 | 7200     | *                 |
| 9215.586   | 16/08/93 |                  | 8.4              | LWP 26157 | 7200     | small aperture, * |
| 9215.704   | 16/08/93 | 7.530            | 8.4              | LWP 26158 | 12598    | *                 |
| 9215.704   | 16/08/93 |                  | 8.4              | LWP 26158 | 12598    | small aperture, * |
| 9217.575   | 18/08/93 | 7.664            | 8.4              | LWP 26168 | 2400     | *                 |
| 9217.648   | 18/08/93 | 7.677            | 8.4              | LWP 26169 | 16197    | *                 |
| 9217.648   | 18/08/93 |                  | 8.4              | LWP 26169 | 16197    | small aperture, * |

TABLE 1. (continued)

| JD-2440000 | Date     | $V_{\text{FES}}$ | $V_{\text{AFJ}}$ | Image No. | Exp. (s) | Notes |
|------------|----------|------------------|------------------|-----------|----------|-------|
| 9427.989   | 16/03/93 | 7.817            | 7.8              | LWP 27711 | 7200     | *     |
| 9428.098   | 16/03/93 | 7.598            | 7.9              | LWP 27712 | 7200     | *     |
| 9428.205   | 16/03/93 | 7.170            | 7.9              | LWP 27713 | 6900     | *     |
| 9436.999   | 25/03/94 | 9.898            | 11.7             | LWP 27761 | 5400     | *     |
| 9437.093   | 25/03/94 | 9.137            | 11.7             | LWP 27762 | 10799    | *     |
| 9437.246   | 25/03/94 | 8.292            | 11.7             | LWP 27763 | 3360     | *     |
| 9449.920   | 07/04/94 |                  | 13.9             | LWP 27836 | 3600     | *     |
| 9449.991   | 07/04/94 |                  | 13.9             | LWP 27837 | 9000     | *     |
| 9450.094   | 07/04/94 |                  | 13.9             | LWP 27838 | 9000     | *     |
| 9455.931   | 13/04/94 |                  | 13.5             | LWP 27893 | 7200     | *     |
| 9456.037   | 13/04/94 |                  | 13.5             | LWP 27894 | 14100    | *     |
| 9508.761   | 05/06/94 | 10.309           | 11.1             | LWP 28326 | 7200     | *     |
| 9508.868   | 05/06/94 | 10.409           | 11.1             | LWP 28327 | 14400    | *     |
| 9537.655   | 04/07/94 | 8.647            | 8.7              | LWP 28539 | 10800    | *     |
| 9537.783   | 04/07/94 | 8.621            | 8.7              | SWP 51308 | 14400    |       |
| 9539.656   | 06/07/94 | 8.642            | 8.6              | LWP 28557 | 10800    | *     |
| 9539.784   | 06/07/94 | 8.613            | 8.6              | SWP 51333 | 14400    |       |

Notes to Table 1.

Some of the LWP low dispersion spectra taken after 1992 Nov 12 (\*) are contaminated by scattered solar spectrum.

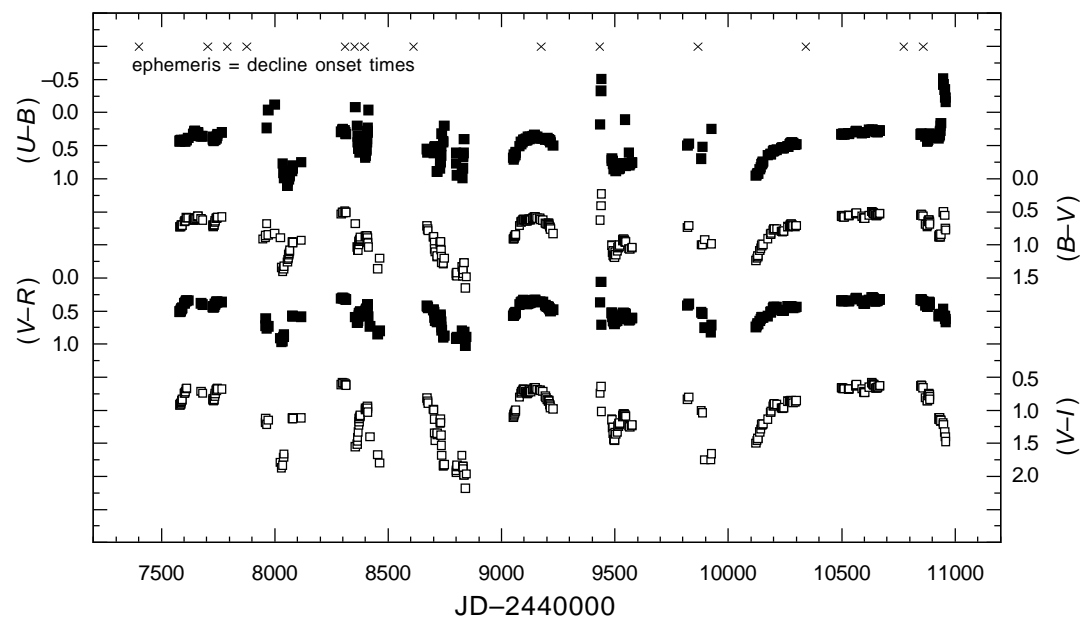


TABLE 2. SAAO  $UBVR_cI_c$  photometry of V854 Centauri.

| Year/JD  | $V$    | $(B-V)$ | $(U-B)$ | $(V-R)$ | $(V-I)$ | Year/JD  | $V$    | $(B-V)$ | $(U-B)$ | $(V-R)$ | $(V-I)$ |
|----------|--------|---------|---------|---------|---------|----------|--------|---------|---------|---------|---------|
| 1989     |        |         |         |         |         |          |        |         |         |         |         |
| 7580.573 | 7.869  | 0.729   | 0.424   | 0.510   | 0.917   | 7651.385 | 7.479  | 0.599   | 0.347   |         |         |
| 7581.596 | 7.894  | 0.729   | 0.436   | 0.510   | 0.924   | 7652.374 | 7.465  | 0.602   | 0.316   |         |         |
| 7584.621 | 7.915  | 0.727   | 0.419   | 0.501   | 0.902   | 7657.326 | 7.400  | 0.581   | 0.312   |         |         |
| 7585.621 | 7.923  | 0.716   | 0.422   | 0.494   | 0.905   | 7660.290 | 7.336  | 0.566   | 0.296   |         |         |
| 7586.617 | 7.907  | 0.705   | 0.418   | 0.482   | 0.888   | 7661.314 | 7.309  | 0.564   | 0.313   |         |         |
| 7588.577 | 7.894  | 0.707   | 0.423   | 0.471   | 0.868   | 7675.491 | 7.440  | 0.601   | 0.358   | 0.385   | 0.716   |
| 7589.544 | 7.878  | 0.704   | 0.421   | 0.466   | 0.863   | 7681.451 | 7.466  | 0.627   | 0.359   | 0.401   | 0.742   |
| 7590.529 | 7.878  | 0.701   | 0.422   | 0.455   | 0.850   | 7727.243 | 8.198  | 0.697   | 0.37    | 0.432   | 0.824   |
| 7591.584 | 7.872  | 0.703   | 0.426   | 0.452   | 0.837   | 7728.242 | 8.212  | 0.705   | 0.402   | 0.436   | 0.838   |
| 7601.599 | 7.673  | 0.650   | 0.418   | 0.381   | 0.741   | 7729.270 | 8.229  | 0.721   | 0.411   | 0.445   | 0.850   |
| 7602.593 | 7.657  | 0.629   | 0.432   | 0.385   | 0.740   | 7730.275 | 8.208  | 0.709   | 0.427   | 0.445   | 0.852   |
| 7605.593 | 7.576  | 0.636   | 0.44    | 0.361   | 0.721   | 7731.245 | 8.162  | 0.706   | 0.416   | 0.438   | 0.843   |
| 7609.581 | 7.452  | 0.588   | 0.42    | 0.347   | 0.673   | 7732.303 | 8.123  | 0.698   | 0.409   | 0.438   | 0.834   |
| 7611.567 | 7.43   | 0.594   | 0.41    | 0.338   | 0.664   | 7735.277 | 7.899  | 0.661   | 0.403   | 0.402   | 0.788   |
| 7618.474 | 7.362  | 0.593   | 0.380   | 0.338   |         | 7737.299 | 7.746  | 0.634   | 0.409   | 0.392   | 0.750   |
| 7641.318 | 7.588  | 0.624   | 0.324   |         |         | 7741.257 | 7.499  | 0.594   | 0.378   | 0.365   | 0.700   |
| 7642.337 | 7.579  | 0.620   | 0.323   |         |         | 7742.241 | 7.453  | 0.601   | 0.390   | 0.369   | 0.698   |
| 7643.353 | 7.563  | 0.615   | 0.314   |         |         | 7744.234 | 7.334  | 0.590   | 0.354   | 0.360   | 0.682   |
| 7645.340 | 7.565  | 0.612   | 0.315   |         |         | 7746.253 | 7.356  | 0.589   | 0.350   | 0.365   | 0.670   |
| 7646.312 | 7.534  | 0.604   | 0.280   |         |         | 7747.242 | 7.34   | 0.584   | 0.323   | 0.357   | 0.679   |
| 7647.298 | 7.528  | 0.607   | 0.284   |         |         | 7767.241 | 7.315  | 0.577   | 0.299   | 0.362   | 0.678   |
| 7648.366 | 7.515  | 0.597   | 0.283   |         |         |          |        |         |         |         |         |
| 1990     |        |         |         |         |         |          |        |         |         |         |         |
| 7946.617 | 14.56  | 0.91    |         |         |         | 8055.345 | 10.59  | 1.26    | 1.11    |         |         |
| 7958.592 | 14.59  | 0.89    |         |         | 1.19    | 8057.344 | 10.40  | 1.22    | 1.04    |         |         |
| 7959.622 | 14.52  | 0.86    |         | 0.72    | 1.18    | 8060.290 | 10.14  | 1.20    | 1.00    |         |         |
| 7960.605 | 14.55  |         |         | 0.61    | 1.12    | 8061.332 | 10.05  | 1.15    | 1.01    |         |         |
| 7963.619 | 14.47  | 0.68    | 0.23    | 0.76    | 1.21    | 8063.340 | 9.91   | 1.130   | 0.967   |         |         |
| 7971.626 | 14.62  | 0.85    | -0.04   | 0.73    | 1.15    | 8065.272 | 9.75   | 1.106   | 0.962   |         |         |
| 7999.465 | 14.61  | 0.83    | -0.12   |         |         | 8066.336 | 9.69   | 1.079   | 0.942   |         |         |
| 8024.534 | 14.02  | 0.89    |         | 0.91    | 1.79    | 8077.299 | 9.051  | 0.956   | 0.880   | 0.573   | 1.123   |
| 8029.386 | 13.29  | 1.34    |         | 0.97    | 1.87    | 8078.301 | 9.035  | 0.962   | 0.805   | 0.575   | 1.117   |
| 8034.438 | 12.55  | 1.40    | 0.77    | 0.96    | 1.83    | 8079.361 | 9.025  | 0.965   | 0.846   | 0.582   | 1.124   |
| 8038.399 | 12.04  | 1.36    | 0.91    | 0.89    | 1.71    | 8116.221 | 8.816  | 0.929   | 0.750   | 0.589   | 1.115   |
| 8040.488 | 11.76  | 1.32    | 0.99    | 0.86    | 1.66    |          |        |         |         |         |         |
| 1991     |        |         |         |         |         |          |        |         |         |         |         |
| 8293.615 | 7.159  | 0.534   | 0.288   | 0.312   | 0.611   | 8374.464 | 10.492 | 0.92    | 0.60    | 0.529   | 1.103   |
| 8297.586 | 7.144  | 0.505   | 0.262   | 0.303   | 0.585   | 8375.570 | 10.333 | 0.91    | 0.53    | 0.51    | 1.086   |
| 8299.611 | 7.143  | 0.514   | 0.250   | 0.300   | 0.586   | 8376.477 | 10.293 | 0.88    | 0.57    | 0.515   | 1.076   |
| 8301.565 | 7.136  | 0.511   | 0.274   | 0.306   | 0.590   | 8398.384 | 9.879  | 0.872   | 0.680   | 0.515   | 0.997   |
| 8308.624 | 7.128  | 0.491   | 0.264   | 0.314   | 0.594   | 8400.431 | 10.091 | 0.869   | 0.651   | 0.493   | 0.970   |
| 8311.558 | 7.157  | 0.507   | 0.294   | 0.320   | 0.603   | 8403.373 | 10.719 | 0.870   | 0.57    | 0.481   | 0.973   |
| 8312.570 | 7.163  | 0.507   | 0.323   | 0.320   | 0.612   | 8404.444 | 10.980 | 0.861   | 0.55    | 0.472   | 0.971   |
| 8313.532 | 7.184  | 0.508   | 0.326   | 0.330   | 0.621   | 8405.374 | 11.285 | 0.867   | 0.45    | 0.465   | 0.967   |
| 8354.505 | 14.12  | 0.68    | -0.08   | 0.59    | 1.55    | 8406.342 | 11.70  | 0.865   | 0.40    | 0.470   | 0.985   |
| 8363.494 | 12.95  | 1.03    | 0.20    | 0.68    | 1.51    | 8408.362 | 12.72  | 0.89    | 0.30    | 0.40    | 0.94    |
| 8364.566 | 12.50  | 1.06    | 0.36    | 0.68    | 1.47    | 8409.354 | 13.36  | 0.96    | 0.28    | 0.40    | 0.97    |
| 8365.529 | 12.13  | 1.08    | 0.45    | 0.66    | 1.41    | 8410.377 | 13.97  | 0.97    | 0.23    | 0.44    | 1.03    |
| 8368.508 | 11.510 | 1.080   | 0.544   | 0.648   | 1.328   | 8412.421 | 14.6   | 1.03    | -0.04   | 0.58    |         |
| 8370.569 | 11.153 | 0.999   | 0.543   | 0.583   | 1.220   | 8419.380 | 14.9   |         |         | 0.73    | 1.40    |
| 8371.500 | 10.974 | 0.950   | 0.541   | 0.562   | 1.176   | 8454.236 | 14.9   | 1.36    |         | 0.85    | 1.67    |
| 8372.557 | 10.790 | 0.938   | 0.534   | 0.538   | 1.127   | 8462.269 | 14.58  | 1.2     |         | 0.8     | 1.8     |

TABLE 2. (continued)

| Year/JD  | <i>V</i> | ( <i>B</i> – <i>V</i> ) | ( <i>U</i> – <i>B</i> ) | ( <i>V</i> – <i>R</i> ) | ( <i>V</i> – <i>I</i> ) | Year/JD  | <i>V</i> | ( <i>B</i> – <i>V</i> ) | ( <i>U</i> – <i>B</i> ) | ( <i>V</i> – <i>R</i> ) | ( <i>V</i> – <i>I</i> ) |
|----------|----------|-------------------------|-------------------------|-------------------------|-------------------------|----------|----------|-------------------------|-------------------------|-------------------------|-------------------------|
| 1992     |          |                         |                         |                         |                         |          |          |                         |                         |                         |                         |
| 8671.606 | 8.202    | 0.712                   | 0.551                   | 0.422                   | 0.815                   | 8742.485 | 13.31    | 1.29                    | 0.45                    | 0.90                    | 1.84                    |
| 8674.574 | 8.555    | 0.760                   | 0.605                   | 0.436                   | 0.861                   | 8743.499 | 13.49    | 1.28                    | 0.43                    | 0.88                    | 1.83                    |
| 8675.598 | 8.698    | 0.786                   | 0.592                   | 0.450                   | 0.891                   | 8747.463 | 13.93    | 1.20                    | 0.20                    | 0.87                    | 1.82                    |
| 8699.616 | 9.783    | 0.881                   | 0.580                   | 0.478                   | 0.985                   | 8799.363 | 13.70    | 1.46                    | 0.61                    | 0.92                    | 1.94                    |
| 8700.552 | 9.935    | 0.878                   | 0.608                   | 0.488                   | 0.997                   | 8800.296 | 13.59    | 1.43                    | 0.77                    | 0.91                    | 1.91                    |
| 8703.578 | 10.735   | 0.960                   | 0.55                    | 0.520                   | 1.135                   | 8802.360 | 13.26    | 1.47                    |                         | 0.92                    | 1.85                    |
| 8705.549 | 11.390   | 1.062                   | 0.52                    | 0.603                   | 1.344                   | 8803.253 | 13.10    | 1.42                    | 0.95                    | 0.89                    | 1.83                    |
| 8706.559 | 11.678   | 1.106                   | 0.51                    | 0.650                   | 1.458                   | 8825.272 | 12.27    | 1.33                    | 0.90                    | 0.80                    | 1.68                    |
| 8715.572 | 10.548   | 1.180                   | 0.888                   | 0.670                   | 1.373                   | 8828.255 | 12.79    | 1.47                    | 0.99                    | 0.88                    | 1.85                    |
| 8716.594 | 10.408   | 1.168                   | 0.892                   | 0.660                   | 1.349                   | 8829.255 | 12.89    | 1.40                    | 0.84                    | 0.87                    | 1.85                    |
| 8728.538 | 10.449   | 0.997                   | 0.84                    | 0.591                   | 1.191                   | 8830.259 | 13.08    | 1.43                    | 0.67                    | 0.87                    | 1.85                    |
| 8729.520 | 10.572   | 0.950                   | 0.77                    | 0.587                   | 1.176                   | 8831.255 | 13.28    | 1.37                    | 0.66                    | 0.86                    | 1.89                    |
| 8730.458 | 10.710   | 0.961                   | 0.75                    | 0.560                   | 1.13                    | 8833.249 | 13.68    | 1.27                    | 0.61                    | 0.86                    | 1.98                    |
| 8731.533 | 11.032   | 0.950                   | 0.75                    | 0.585                   | 1.187                   | 8834.262 | 13.83    | 1.27                    | 0.40                    | 0.82                    | 1.98                    |
| 8733.490 | 11.884   | 1.078                   | 0.65                    | 0.658                   | 1.377                   | 8840.234 | 13.78    | 1.65                    |                         | 1.02                    | 2.18                    |
| 8734.535 | 12.35    | 1.17                    | 0.51                    | 0.74                    | 1.53                    | 8844.245 | 13.37    | 1.48                    |                         | 0.89                    | 1.96                    |
| 8735.504 | 12.73    | 1.27                    | 0.32                    | 0.79                    | 1.68                    |          |          |                         |                         |                         |                         |
| 1993     |          |                         |                         |                         |                         |          |          |                         |                         |                         |                         |
| 9051.621 | 8.832    | 0.911                   | 0.68                    | 0.571                   | 1.105                   | 9125.430 | 7.445    | 0.619                   | 0.367                   | 0.372                   | 0.712                   |
| 9053.610 | 8.752    | 0.91                    | 0.71                    | 0.57                    | 1.09                    | 9126.378 | 7.438    | 0.614                   | 0.375                   | 0.367                   | 0.707                   |
| 9055.621 | 8.680    | 0.902                   | 0.64                    | 0.555                   | 1.065                   | 9128.395 | 7.457    | 0.619                   | 0.377                   | 0.370                   | 0.721                   |
| 9056.569 | 8.645    | 0.881                   | 0.670                   | 0.546                   | 1.045                   | 9137.336 | 7.424    | 0.600                   | 0.37                    | 0.359                   | 0.692                   |
| 9057.629 | 8.610    | 0.871                   | 0.642                   | 0.540                   | 1.045                   | 9138.370 | 7.414    | 0.597                   | 0.356                   | 0.357                   | 0.683                   |
| 9060.542 | 8.498    | 0.860                   | 0.637                   | 0.529                   | 1.013                   | 9139.375 | 7.397    | 0.590                   | 0.368                   | 0.350                   | 0.674                   |
| 9061.544 | 8.460    | 0.853                   | 0.60                    | 0.524                   | 1.011                   | 9143.314 | 7.371    | 0.576                   | 0.35                    | 0.340                   | 0.657                   |
| 9062.556 | 8.421    | 0.843                   | 0.606                   | 0.519                   | 0.995                   | 9145.360 | 7.372    | 0.580                   | 0.34                    | 0.332                   | 0.661                   |
| 9079.494 | 7.849    | 0.708                   | 0.508                   | 0.402                   | 0.800                   | 9149.344 | 7.373    | 0.573                   | 0.365                   | 0.331                   | 0.655                   |
| 9086.607 | 7.719    | 0.656                   | 0.44                    | 0.368                   | 0.745                   | 9156.307 | 7.386    | 0.595                   | 0.366                   | 0.358                   | 0.685                   |
| 9087.531 | 7.68     | 0.64                    | 0.48                    | 0.36                    | 0.72                    | 9168.309 | 7.399    | 0.596                   | 0.392                   | 0.360                   | 0.693                   |
| 9092.466 | 7.62     | 0.621                   | 0.443                   | 0.352                   | 0.695                   | 9172.303 | 7.439    | 0.617                   | 0.391                   | 0.365                   | 0.700                   |
| 9096.478 | 7.562    | 0.621                   | 0.412                   | 0.337                   | 0.681                   | 9181.322 | 7.500    | 0.626                   | 0.39                    | 0.36                    | 0.712                   |
| 9097.447 | 7.559    | 0.613                   | 0.418                   | 0.346                   | 0.683                   | 9193.252 | 7.761    | 0.670                   | 0.412                   | 0.409                   | 0.788                   |
| 9098.477 | 7.556    | 0.618                   | 0.417                   | 0.347                   | 0.692                   | 9196.242 | 7.827    | 0.678                   | 0.394                   | 0.426                   | 0.810                   |
| 9104.478 | 7.553    | 0.633                   | 0.412                   | 0.373                   | 0.720                   | 9202.240 | 7.988    | 0.683                   | 0.382                   | 0.432                   | 0.842                   |
| 9106.419 | 7.536    | 0.625                   | 0.418                   | 0.371                   | 0.722                   | 9206.230 | 8.066    | 0.672                   | 0.404                   | 0.444                   | 0.855                   |
| 9108.427 | 7.577    | 0.622                   | 0.396                   | 0.377                   | 0.725                   | 9207.236 | 8.082    | 0.670                   | 0.408                   | 0.435                   | 0.852                   |
| 9111.478 | 7.568    | 0.629                   | 0.411                   | 0.386                   | 0.739                   | 9208.250 | 8.100    | 0.680                   | 0.410                   | 0.445                   | 0.855                   |
| 9112.407 | 7.528    | 0.637                   | 0.420                   | 0.393                   | 0.750                   | 9209.225 | 8.123    | 0.694                   | 0.411                   | 0.451                   | 0.862                   |
| 9113.384 | 7.510    | 0.636                   | 0.40                    | 0.389                   | 0.742                   | 9212.233 | 8.230    | 0.712                   | 0.417                   | 0.461                   | 0.901                   |
| 9115.373 | 7.499    | 0.620                   | 0.400                   | 0.386                   | 0.738                   | 9213.232 | 8.271    | 0.728                   | 0.42                    | 0.475                   | 0.916                   |
| 9117.396 | 7.475    | 0.619                   | 0.37                    | 0.385                   | 0.727                   | 9214.234 | 8.316    | 0.737                   | 0.419                   | 0.487                   | 0.939                   |
| 9120.412 | 7.454    | 0.612                   | 0.39                    | 0.372                   | 0.716                   | 9216.237 | 8.400    | 0.760                   | 0.449                   | 0.501                   | 0.965                   |
| 9122.428 | 7.443    | 0.615                   | 0.382                   | 0.374                   | 0.708                   | 9227.273 | 8.593    | 0.831                   | 0.50                    | 0.480                   | 0.980                   |
| 9124.458 | 7.434    | 0.610                   | 0.396                   | 0.346                   | 0.696                   |          |          |                         |                         |                         |                         |
| 1994     |          |                         |                         |                         |                         |          |          |                         |                         |                         |                         |
| 9434.547 | 9.707    | 0.627                   | 0.180                   | 0.367                   | 0.745                   | 9518.340 | 10.174   | 1.011                   | 0.846                   | 0.605                   | 1.204                   |
| 9438.584 | 12.41    | 0.41                    | -0.33                   | 0.06                    | 0.64                    | 9519.350 | 10.132   | 1.015                   | 0.845                   | 0.606                   | 1.203                   |
| 9440.514 | 13.41    | 0.23                    | -0.51                   | 0.71                    | 1.02                    | 9520.335 | 10.061   | 1.004                   | 0.839                   | 0.601                   | 1.195                   |
| 9485.413 | 11.348   | 1.002                   | 0.724                   | 0.531                   | 1.137                   | 9534.265 | 9.187    | 0.935                   | 0.799                   | 0.558                   | 1.096                   |
| 9486.392 | 11.332   | 1.006                   | 0.69                    | 0.528                   | 1.145                   | 9535.253 | 9.137    | 0.927                   | 0.795                   | 0.553                   | 1.082                   |
| 9489.389 | 11.763   | 1.112                   | 0.73                    | 0.585                   | 1.259                   | 9537.279 | 9.048    | 0.917                   | 0.774                   | 0.537                   | 1.061                   |
| 9490.392 | 11.798   | 1.085                   | 0.729                   | 0.578                   | 1.256                   | 9538.266 | 9.020    | 0.916                   | 0.774                   | 0.530                   | 1.054                   |

TABLE 2. (continued)

| Year/JD         | <i>V</i> | ( <i>B</i> – <i>V</i> ) | ( <i>U</i> – <i>B</i> ) | ( <i>V</i> – <i>R</i> ) | ( <i>V</i> – <i>I</i> ) | Year/JD   | <i>V</i> | ( <i>B</i> – <i>V</i> ) | ( <i>U</i> – <i>B</i> ) | ( <i>V</i> – <i>R</i> ) | ( <i>V</i> – <i>I</i> ) |
|-----------------|----------|-------------------------|-------------------------|-------------------------|-------------------------|-----------|----------|-------------------------|-------------------------|-------------------------|-------------------------|
| 1994 continued. |          |                         |                         |                         |                         |           |          |                         |                         |                         |                         |
| 9492.388        | 11.92    | 1.158                   | 0.78                    | 0.646                   | 1.355                   | 9539.331  | 9.014    | 0.919                   | 0.767                   | 0.535                   | 1.061                   |
| 9495.389        | 12.08    | 1.17                    | 0.85                    | 0.67                    | 1.44                    | 9540.279  | 9.017    | 0.926                   | 0.775                   | 0.536                   | 1.058                   |
| 9497.424        | 11.954   |                         |                         | 0.693                   | 1.453                   | 9541.279  | 9.023    | 0.929                   | 0.771                   | 0.538                   | 1.061                   |
| 9498.362        | 11.950   | 1.190                   |                         | 0.668                   | 1.445                   | 9544.360  | 9.044    | 0.946                   | 0.794                   | 0.542                   | 1.071                   |
| 9501.423        | 11.52    | 1.104                   | 0.84                    | 0.632                   | 1.337                   | 9545.280  | 9.058    | 0.954                   | 0.106                   | 0.540                   | 1.070                   |
| 9503.418        | 11.472   | 1.149                   | 0.880                   | 0.659                   | 1.362                   | 9546.283  | 9.085    | 0.953                   | 0.805                   | 0.551                   | 1.085                   |
| 9510.340        | 10.966   | 1.094                   | 0.840                   | 0.649                   | 1.331                   | 9547.293  | 9.086    | 0.955                   | 0.798                   | 0.547                   | 1.090                   |
| 9513.331        | 10.579   | 1.038                   | 0.824                   | 0.613                   | 1.243                   | 9562.236  | 9.619    | 1.058                   | 0.607                   | 0.638                   | 1.236                   |
| 9514.336        | 10.500   | 1.035                   | 0.837                   | 0.617                   | 1.243                   | 9563.235  | 9.649    | 1.058                   | 0.795                   | 0.634                   | 1.233                   |
| 9515.312        | 10.422   | 1.043                   | 0.858                   | 0.616                   | 1.242                   | 9566.231  | 9.768    | 1.061                   | 0.778                   | 0.632                   | 1.249                   |
| 9516.316        | 10.328   | 1.032                   | 0.848                   | 0.607                   | 1.226                   | 9574.241  | 9.895    | 1.047                   | 0.758                   | 0.609                   | 1.231                   |
| 9517.359        | 10.246   | 1.022                   | 0.845                   | 0.606                   | 1.211                   | 9575.238  | 9.881    | 1.036                   | 0.756                   | 0.603                   | 1.222                   |
| 1995            |          |                         |                         |                         |                         |           |          |                         |                         |                         |                         |
| 9820.513        | 7.910    | 0.736                   | 0.496                   | 0.419                   | 0.836                   | 9896.342  | 14.79    | 0.92                    |                         | 0.75                    | 1.75                    |
| 9825.572        | 7.837    | 0.706                   | 0.470                   | 0.393                   | 0.801                   | 9923.275  | 14.94    |                         |                         | 0.82                    | 1.75                    |
| 9880.327        | 11.076   | 0.996                   | 0.695                   | 0.521                   | 1.005                   | 9926.301  | 14.802   | 0.983                   | 0.248                   | 0.713                   | 1.657                   |
| 1996            |          |                         |                         |                         |                         |           |          |                         |                         |                         |                         |
| 10121.613       | 10.300   | 1.233                   | 0.951                   | 0.740                   | 1.499                   | 10237.354 | 8.272    | 0.797                   | 0.534                   | 0.488                   | 0.968                   |
| 10126.592       | 10.152   | 1.202                   | 0.935                   | 0.717                   | 1.461                   | 10238.303 | 8.274    | 0.793                   | 0.539                   | 0.492                   | 0.974                   |
| 10129.618       | 10.057   | 1.180                   | 0.923                   | 0.692                   | 1.429                   | 10239.285 | 8.272    | 0.802                   | 0.525                   | 0.493                   | 0.968                   |
| 10130.615       | 10.058   | 1.164                   | 0.917                   | 0.694                   | 1.423                   | 10244.327 | 8.273    | 0.794                   | 0.530                   | 0.494                   | 0.967                   |
| 10138.625       | 9.757    | 1.084                   | 0.855                   | 0.650                   | 1.327                   | 10245.282 | 8.265    | 0.790                   | 0.531                   | 0.493                   | 0.962                   |
| 10142.545       | 9.599    | 1.053                   | 0.825                   | 0.619                   | 1.284                   | 10262.273 | 8.065    | 0.720                   | 0.515                   | 0.428                   | 0.866                   |
| 10147.544       | 9.426    | 1.011                   | 0.777                   | 0.596                   | 1.224                   | 10263.270 | 8.068    | 0.728                   | 0.514                   | 0.431                   | 0.862                   |
| 10148.585       | 9.385    | 0.997                   | 0.779                   | 0.590                   | 1.211                   | 10270.258 | 8.078    | 0.719                   | 0.479                   | 0.437                   | 0.865                   |
| 10149.573       | 9.365    | 0.992                   | 0.759                   | 0.591                   | 1.213                   | 10272.268 | 8.051    | 0.702                   | 0.486                   | 0.431                   | 0.858                   |
| 10152.497       | 9.310    | 0.992                   | 0.740                   | 0.595                   | 1.208                   | 10273.264 | 8.066    | 0.702                   | 0.472                   | 0.426                   | 0.857                   |
| 10173.517       | 8.919    | 0.908                   | 0.644                   | 0.579                   | 1.137                   | 10275.230 | 8.027    | 0.699                   | 0.470                   | 0.433                   | 0.864                   |
| 10186.512       | 8.631    | 0.838                   | 0.630                   | 0.518                   | 1.035                   | 10276.227 | 8.016    | 0.701                   | 0.458                   | 0.440                   | 0.867                   |
| 10188.493       | 8.572    | 0.824                   | 0.624                   | 0.506                   | 1.013                   | 10277.247 | 7.994    | 0.686                   | 0.459                   | 0.435                   | 0.856                   |
| 10197.292       | 8.355    | 0.775                   | 0.584                   | 0.457                   | 0.939                   | 10280.233 | 7.964    | 0.697                   | 0.454                   | 0.437                   | 0.865                   |
| 10199.498       | 8.324    | 0.772                   | 0.579                   | 0.453                   | 0.932                   | 10281.224 | 7.962    | 0.700                   | 0.451                   | 0.436                   | 0.865                   |
| 10201.441       | 8.273    | 0.760                   | 0.578                   | 0.443                   | 0.911                   | 10285.224 | 7.975    | 0.714                   | 0.465                   | 0.457                   | 0.887                   |
| 10202.475       | 8.239    | 0.755                   | 0.570                   | 0.436                   | 0.902                   | 10295.230 | 7.908    | 0.724                   | 0.483                   | 0.447                   | 0.877                   |
| 10213.432       | 8.210    | 0.758                   | 0.561                   | 0.444                   | 0.913                   | 10299.258 | 7.862    | 0.706                   | 0.478                   | 0.435                   | 0.854                   |
| 10234.361       | 8.264    | 0.796                   | 0.535                   | 0.487                   | 0.965                   |           |          |                         |                         |                         |                         |
| 1997            |          |                         |                         |                         |                         |           |          |                         |                         |                         |                         |
| 10499.586       | 7.404    | 0.560                   | 0.329                   | 0.344                   | 0.667                   | 10600.299 | 7.420    | 0.602                   | 0.296                   | 0.382                   | 0.731                   |
| 10500.624       | 7.399    | 0.566                   | 0.326                   | 0.344                   | 0.658                   | 10601.387 | 7.431    | 0.598                   | 0.298                   | 0.389                   | 0.733                   |
| 10503.621       | 7.405    | 0.567                   | 0.325                   | 0.344                   | 0.672                   | 10619.348 | 7.338    | 0.551                   | 0.256                   | 0.334                   | 0.651                   |
| 10506.577       | 7.399    | 0.578                   | 0.320                   | 0.350                   | 0.665                   | 10632.313 | 7.187    | 0.496                   | 0.261                   | 0.297                   | 0.581                   |
| 10510.617       | 7.444    | 0.578                   | 0.328                   | 0.351                   | 0.674                   | 10636.333 | 7.191    | 0.503                   | 0.255                   | 0.296                   | 0.597                   |
| 10529.547       | 7.409    | 0.555                   | 0.316                   | 0.352                   | 0.686                   | 10638.330 | 7.210    | 0.514                   | 0.267                   | 0.304                   | 0.607                   |
| 10530.511       | 7.407    | 0.553                   | 0.315                   | 0.352                   | 0.684                   | 10640.284 | 7.226    | 0.519                   | 0.268                   | 0.313                   | 0.617                   |
| 10531.534       | 7.414    | 0.559                   | 0.314                   | 0.350                   | 0.677                   | 10641.295 | 7.225    | 0.525                   | 0.272                   | 0.315                   | 0.613                   |
| 10532.543       | 7.407    | 0.555                   | 0.318                   | 0.346                   | 0.675                   | 10642.294 | 7.235    | 0.532                   | 0.274                   | 0.320                   | 0.616                   |
| 10560.401       | 7.305    | 0.531                   | 0.288                   | 0.316                   | 0.631                   | 10648.355 | 7.294    | 0.553                   | 0.284                   | 0.354                   | 0.665                   |
| 10563.480       | 7.312    | 0.525                   | 0.293                   | 0.315                   | 0.625                   | 10652.285 | 7.319    | 0.560                   | 0.288                   | 0.349                   | 0.666                   |
| 10564.473       | 7.304    | 0.523                   | 0.286                   | 0.309                   | 0.620                   | 10655.276 | 7.308    | 0.546                   | 0.287                   | 0.344                   | 0.662                   |

TABLE 2. (continued)

| Year/JD         | <i>V</i> | ( <i>B</i> − <i>V</i> ) | ( <i>U</i> − <i>B</i> ) | ( <i>V</i> − <i>R</i> ) | ( <i>V</i> − <i>I</i> ) | Year/JD   | <i>V</i> | ( <i>B</i> − <i>V</i> ) | ( <i>U</i> − <i>B</i> ) | ( <i>V</i> − <i>R</i> ) | ( <i>V</i> − <i>I</i> ) |
|-----------------|----------|-------------------------|-------------------------|-------------------------|-------------------------|-----------|----------|-------------------------|-------------------------|-------------------------|-------------------------|
| 1997 continued. |          |                         |                         |                         |                         |           |          |                         |                         |                         |                         |
| 10565.462       | 7.284    | 0.515                   | 0.281                   | 0.304                   | 0.613                   | 10657.269 | 7.309    | 0.541                   | 0.290                   | 0.341                   | 0.655                   |
| 10589.377       | 7.290    | 0.567                   | 0.311                   | 0.346                   | 0.674                   | 10659.241 | 7.317    | 0.541                   | 0.288                   | 0.339                   | 0.653                   |
| 10597.429       | 7.380    | 0.592                   | 0.303                   | 0.375                   | 0.719                   | 10666.291 | 7.293    | 0.531                   | 0.272                   | 0.321                   | 0.632                   |
| 10598.392       | 7.399    | 0.597                   | 0.304                   | 0.384                   | 0.723                   | 10668.279 | 7.299    | 0.526                   | 0.277                   | 0.324                   | 0.629                   |
| 10599.381       | 7.416    | 0.599                   | 0.303                   | 0.387                   | 0.734                   |           |          |                         |                         |                         |                         |
| 1998            |          |                         |                         |                         |                         |           |          |                         |                         |                         |                         |
| 10848.602       | 7.405    | 0.549                   | 0.328                   | 0.327                   | 0.634                   | 10888.597 | 9.215    | 0.686                   | 0.319                   | 0.401                   | 0.835                   |
| 10849.605       | 7.382    | 0.551                   | 0.329                   | 0.330                   | 0.633                   | 10927.540 | 10.771   | 0.879                   | 0.389                   | 0.583                   | 1.142                   |
| 10851.603       | 7.354    | 0.540                   | 0.317                   | 0.323                   | 0.619                   | 10929.487 | 10.793   | 0.865                   | 0.357                   | 0.558                   | 1.112                   |
| 10852.602       | 7.369    | 0.541                   | 0.323                   | 0.330                   | 0.625                   | 10931.499 | 10.945   | 0.849                   | 0.338                   | 0.556                   | 1.112                   |
| 10858.615       | 7.537    | 0.561                   | 0.329                   | 0.351                   | 0.662                   | 10933.423 | 11.198   | 0.884                   | 0.295                   | 0.557                   | 1.141                   |
| 10869.635       | 8.691    | 0.689                   | 0.364                   | 0.412                   | 0.809                   | 10934.498 | 11.344   | 0.882                   | 0.275                   | 0.566                   | 1.151                   |
| 10876.616       | 8.879    | 0.722                   | 0.437                   | 0.431                   | 0.853                   | 10936.430 | 11.635   | 0.869                   | 0.197                   | 0.559                   | 1.167                   |
| 10877.624       | 8.849    | 0.708                   | 0.427                   | 0.431                   | 0.854                   | 10937.448 | 11.819   | 0.837                   | 0.162                   | 0.543                   | 1.155                   |
| 10881.607       | 8.787    | 0.646                   | 0.406                   | 0.388                   | 0.782                   | 10947.444 | 13.516   | 0.515                   | −0.520                  | 0.472                   | 1.187                   |
| 10883.591       | 8.709    | 0.627                   | 0.382                   | 0.366                   | 0.742                   | 10948.432 | 13.622   | 0.498                   | −0.427                  | 0.572                   | 1.217                   |
| 10885.565       | 8.782    | 0.628                   | 0.364                   | 0.372                   | 0.756                   | 10954.486 | 13.511   | 0.553                   | −0.349                  | 0.571                   | 1.328                   |
| 10886.552       | 8.880    | 0.642                   | 0.343                   | 0.376                   | 0.767                   | 10957.414 | 13.218   | 0.752                   | −0.225                  | 0.619                   | 1.399                   |
| 10887.550       | 9.037    | 0.660                   | 0.332                   | 0.383                   | 0.795                   | 10958.432 | 13.131   | 0.777                   | −0.163                  | 0.666                   | 1.472                   |

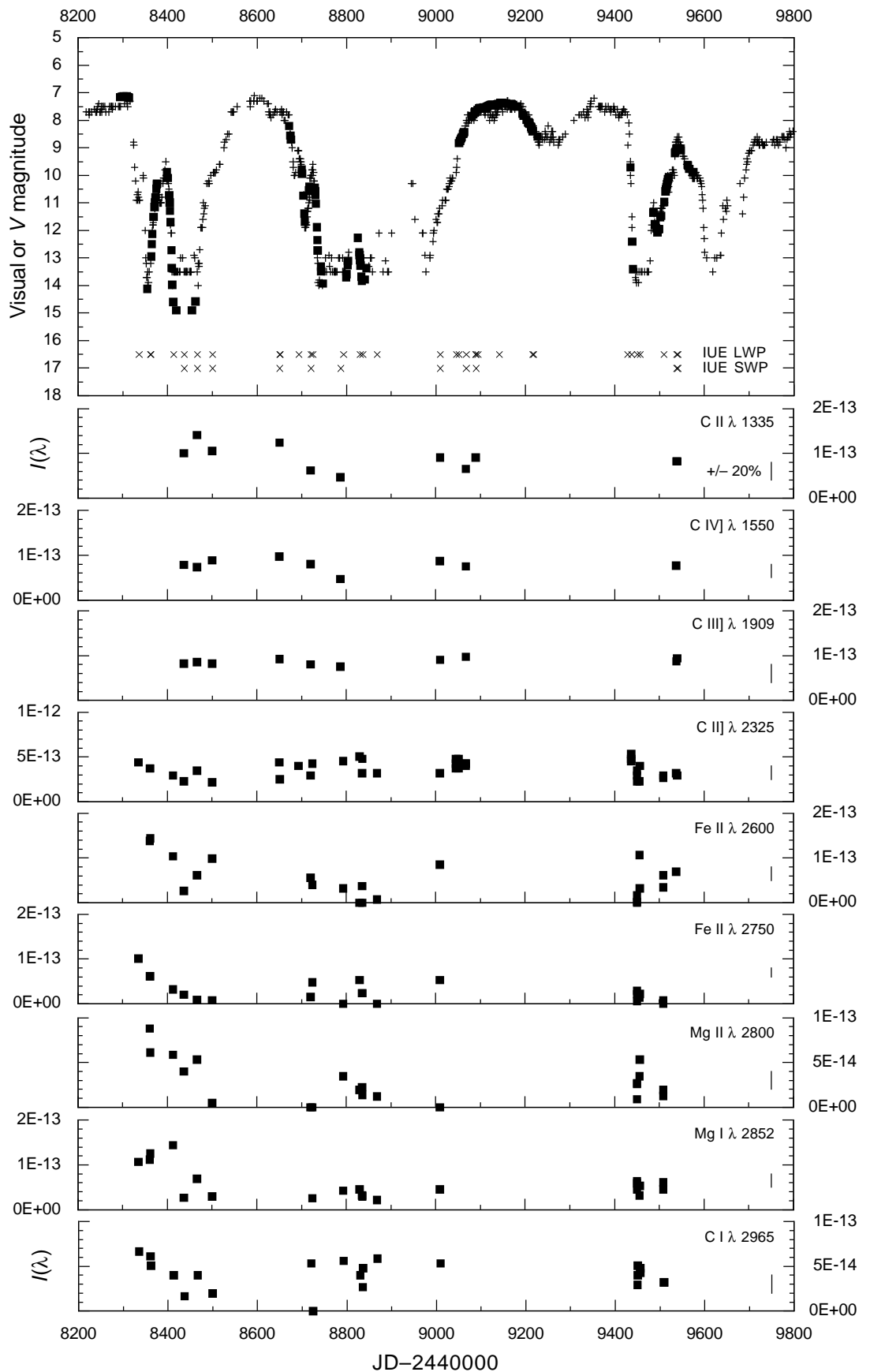


TABLE 3. Emission-line decay times and classification.

| Line                  | 1991 decline<br>$t_{0.5}$ (d) | 1992 decline<br>$t_{0.5}$ (d) | 1994 decline<br>$t_{0.5}$ (d) |     |        |
|-----------------------|-------------------------------|-------------------------------|-------------------------------|-----|--------|
| C II $\lambda$ 1335   | const.                        | BL                            | 95                            | E2  | const. |
| C IV] $\lambda$ 1550  | const.                        | BL                            | long?                         | BL  | const. |
| C III] $\lambda$ 1909 | const.                        | BL                            | const.                        | BL  | const. |
| C II] $\lambda$ 2325  | 200                           | BL                            | const.                        | BL  | 20     |
| Fe II $\lambda$ 2600  | 120                           | E2                            | 75                            | E2  | < 20   |
| Fe II $\lambda$ 2750  | 50                            | E2                            |                               | ?   | < 20   |
| Mg II $\lambda$ 2800  | 50                            | E2                            |                               | E2  | < 20   |
| Mg I $\lambda$ 2852   | 80                            | E2                            |                               | E2  | < 20   |
| C I $\lambda$ 2965    | 100                           | E2                            |                               | E1? | ?      |

Notes to Table 3.

For the definition of E1/E2/BL, see Section 3.4. The emission line decay times given are the times taken for the lines to fade to half the line flux as seen when the star is at maximum light, i.e. the line half-life ( $t_{0.5}$ ).

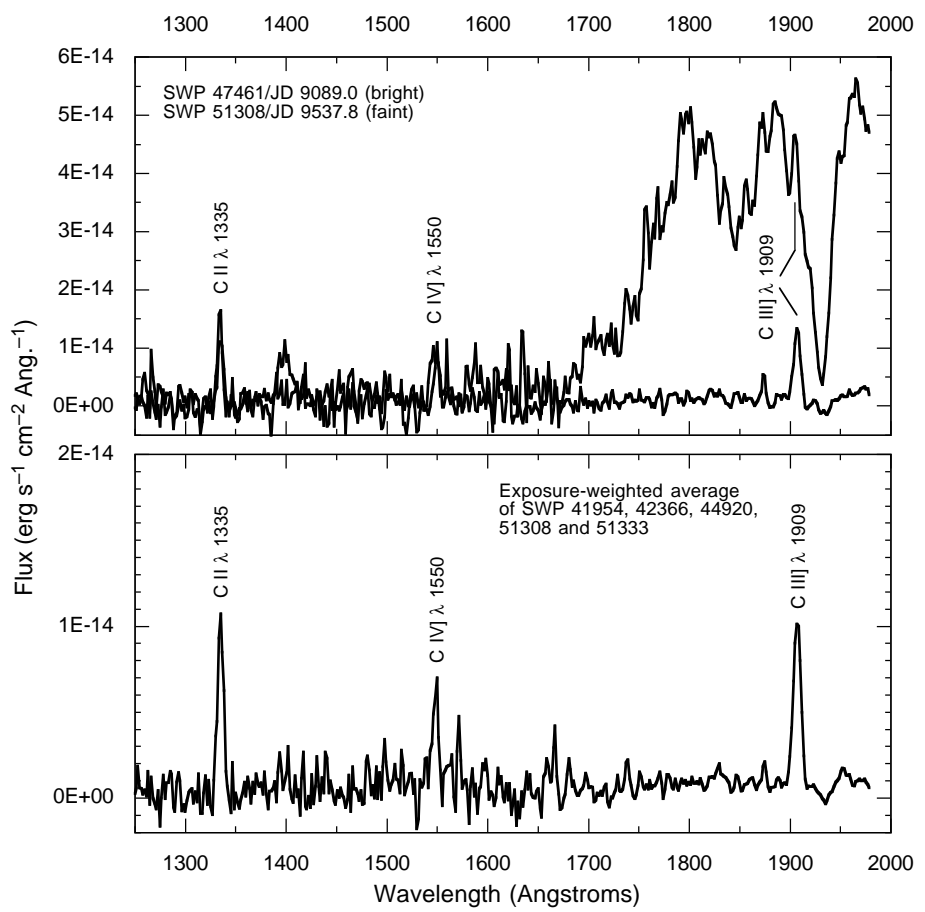


TABLE 4. Decline onset times for V854 Centauri, 1987–1998.

| <i>n</i> | Observed<br>(JD–2400000) | Calculated<br>(JD–2400000) | O–C<br>(d) | reference                    |
|----------|--------------------------|----------------------------|------------|------------------------------|
| –10      | 46970                    | 46968                      | 2          | McNaught (1988)              |
| 0        | 47400                    | 47400                      | 0          | Lawson & Cottrell (1989)     |
| 7        | 47705                    | 47703                      | 2          | Lawson <i>et al.</i> (1992)  |
| 9        | 47785                    | 47790                      | –5         | Lawson <i>et al.</i> (1992)  |
| 11       | 47875                    | 47876                      | –1         | Lawson <i>et al.</i> (1992)  |
| 21       | 48310                    | 48308                      | 2          | Lawson <i>et al.</i> (1992)  |
| 22       | 48350                    | 48352                      | –2         | Lawson <i>et al.</i> (1992)  |
| 23       | 48395                    | 48395                      | 0          | Clayton <i>et al.</i> (1992) |
| 28       | 48610                    | 48611                      | –1         | this paper                   |
| 41       | 49180                    | 49173                      | 7          | this paper                   |
| 47       | 49430                    | 49432                      | –2         | this paper                   |
| 57       | 49860                    | 49865                      | –5         | this paper                   |
| 68       | 50345                    | 50340                      | 5          | this paper                   |
| 78       | 50775                    | 50772                      | 3          | this paper                   |
| 80       | 50855                    | 50859                      | –4         | this paper                   |

Notes to Table 4.

Decline onset times are given by the ephemeris:  $JD_n = 2447400.43 + 43.23n$ .

